Volume 6
Number 12
21 June 2022
Pages 2871–3086

Sustainable Energy & Fuels

Interdisciplinary research for the development of sustainable energy technologies

rsc.li/sustainable-energy

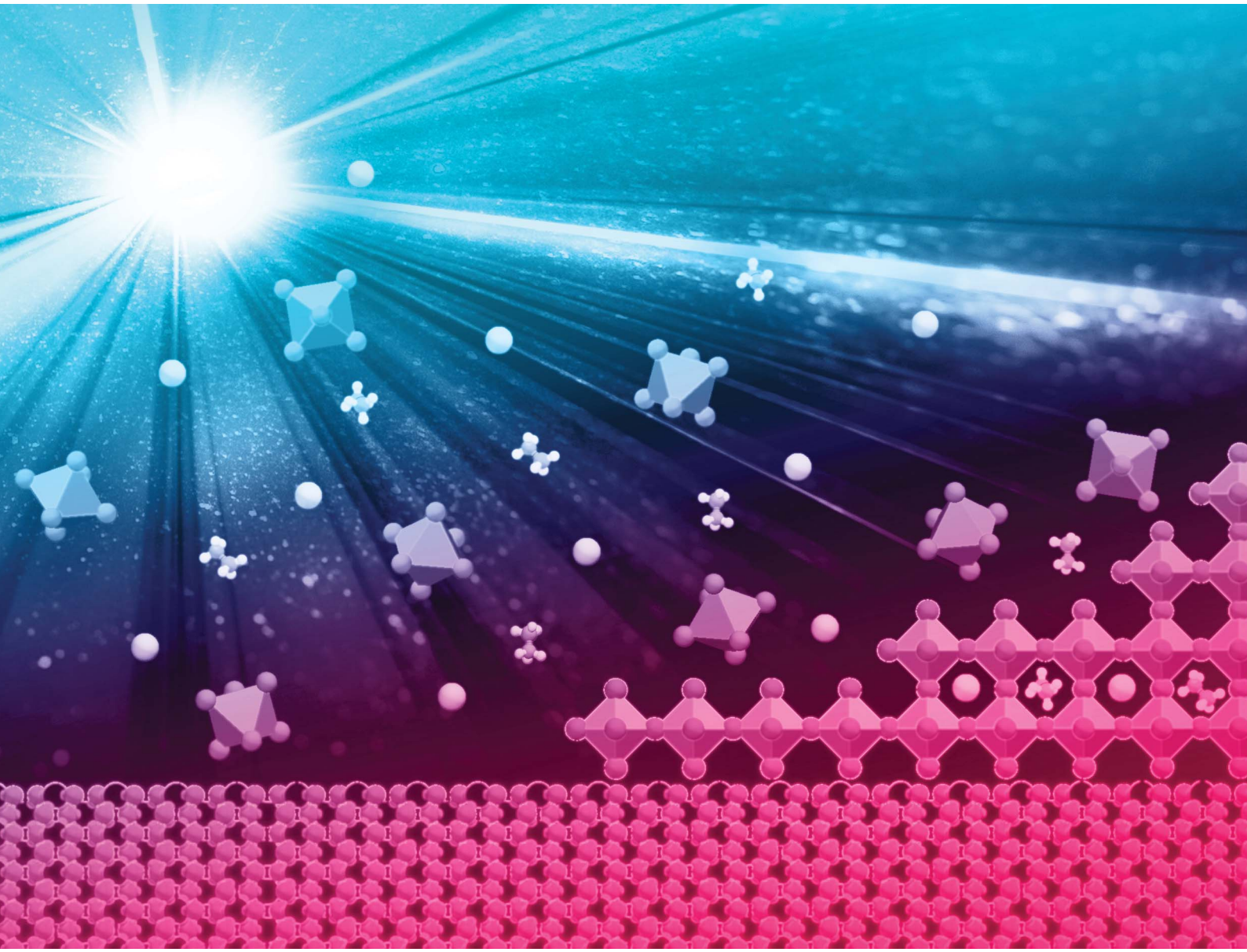

ISSN 2398-4902

ROYAL SOCIETY OF CHEMISTRY

REVIEW ARTICLE

Syed Ghufran Hashmi *et al.*

Recent developments in perovskite-based precursor inks for scalable architectures of perovskite solar cell technology

Sustainable Energy & Fuels

ROYAL SOCIETY OF CHEMISTRY

REVIEW

View Article Online
View Journal | View Issue

Cite this: *Sustainable Energy Fuels*, 2022, **6**, 2879

Recent developments in perovskite-based precursor inks for scalable architectures of perovskite solar cell technology

Ethan Berger,[a] Mohammad Bagheri,[a] Somayyeh Asgari,[b] Jin Zhou,[a] Mikko Kokkonen,[a] Parisa Talebi,[c] Jingshan Luo,[d] Ana Flávia Nogueira,[e] Trystan Watson[f] and Syed Ghufran Hashmi*[a]

Received 4th February 2022
Accepted 2nd May 2022

DOI: 10.1039/d2se00162d

rsc.li/sustainable-energy

The progressive enhancements in solar-to-electrical conversion within the past decade have allowed organic–inorganic lead halide perovskite-based solar cell (PSC) technology to become a competitive candidate for creating affordable and sustainable electricity. This review highlights the developments in fabricating advanced precursor inks of organic–inorganic lead halide perovskite-based light harvesters for large-area perovskite solar cell technology. One of the key characteristics of this promising photovoltaic technology includes solution processing, which offers possibilities to scale up lab-sized solar cell devices into large-area perovskite solar modules comprising unique device architectures. These have been realized in recent years for their deployment in various applications such as building-integrated photovoltaics or internet of things (IoT) devices. In this regard, the presented overview highlights the recent trends that have emerged in the research and development of novel perovskite precursor ink formulations, and it also discusses their contribution toward demonstrating efficient, scalable, and durable PSC technology to create electricity and energize futuristic applications. Various

[a]*Microelectronics Research Unit, Faculty of Information Technology & Electrical Engineering, University of Oulu, P. O. Box 4500, FI-90014, Finland. E-mail: ghufran.hashmi@oulu.fi*

[b]*Optoelectronics and Measurement Techniques Research Unit, Faculty of Information Technology and Electrical Engineering, University of Oulu, Oulu, Finland*

[c]*Nano and Molecular Systems Research Unit, University of Oulu, Finland*

[d]*Institute of Photoelectronic Thin Film Devices and Technology, Solar Energy Research Center, Key Laboratory of Photoelectronic Thin Film Devices and Technology of Tianjin, Ministry of Education Engineering Research Center of Thin Film Photoelectronic Technology, Renewable Energy Conversion and Storage Center, Nankai University, Tianjin 300350, China*

[e]*Laboratory of Nanotechnology and Solar Energy, Chemistry Institute, University of Campinas – UNICAMP, P. O. Box 6154, 13083-970 Campinas, SP, Brazil*

[f]*SPECIFIC, College of Engineering, Baglan Bay Innovation and Knowledge Centre, Swansea University, Baglan SA12 & AX, UK*

Ethan Berger received his bachelor's and master's degrees in physical sciences from the Ecole Polytechnique Fédérale de Lausanne (EPFL), Switzerland. For his master's thesis, he worked on the dielectric response of hybrid halide perovskites. He is currently working as a doctoral researcher in computational physics at the Microelectronics Research Unit (MIC) at the University of Oulu, Finland. His current research focuses on Raman spectroscopy from first-principles calculations, molecular dynamics and machine learning.

Mohammad Bagheri received his master's degree in nanoelectronics engineering from QIAU, Iran. He is currently working as a doctoral researcher in computational materials physics at the Microelectronics Research Unit (MIC) of the Faculty of Information Technology & Electrical Engineering, University of Oulu, Finland. His current research focuses on material modeling and Raman spectroscopy with first-principles calculations, as well as developing high-throughput computations. He is also interested in developing and using materials databases to discover novel materials for energy and quantum technology applications.

reports were included aiming to showcase the robust photovoltaic performance of large-area perovskite solar modules in a variety of device configurations, hence providing a brief overview of the role of state-of-the-art scalable precursor ink development in transforming unstable lab-sized solar cells into robust, low-cost perovskite solar cell technology that can be scaled up to cover much larger areas.

1. Introduction

Since its first report,[1] the rapid escalation of solar-to-electrical conversion over the last decade (Fig. 1)[1–10] has made organic–inorganic lead halide perovskite-based solar cell (PSC) technology a game-changer for creating electricity at an affordable cost.[11] Its key features include solution processing, which offers the possibility of rapid production of perovskite solar modules (PSMs), efficient solar-to-electrical energy conversions under various light intensity conditions,[12,13] and the well-established long term operational stability under various environmental conditions.[12,14–18] Thus, PSC technology has become a unique candidate among other emerging and next-generation-based photovoltaic (PV) technologies[19–22] in the emerging area of building-integrated photovoltaics (BIPV)[23] and for the next generation of maintenance-free IoT devices.[24–26]

This review highlights the developments being made in the fabrication of advanced scalable precursor inks of organic–inorganic lead halide perovskite-based light harvesters for large-area PSC technology. In the past decade of progressive research, various scalable configurations for PSC technology have been developed.[27,28] These have utilized various unique

Somayyeh Asgari received her BSc degree in electrical and power electronics engineering from Zanjan University, Zanjan, Iran, in 2014, and her MSc degree in Telecommunications Engineering from K. N. Toosi University of Technology, Tehran, Iran, in 2017. She is doing her PhD research under the supervision of Professor Tapio Fabritius in the Optoelectronics and Measurement Techniques Research Unit, Faculty of Information Technology and Electrical Engineering, University of Oulu, Oulu, Finland. She is an author and co-author of 23 peer-reviewed journals and 3 conference papers. Her research interests include the design and simulation of solar cells, optical metamaterials, chiral metastructures, graphene plasmonic devices and structures, MEMS metamaterials, and linear and nonlinear plasmonic metal-based devices.

Jin Zhou received his MS degree in Chemical Engineering and Technology from the College of Chemistry, Chemical Engineering and Materials Science, Soochow University, China. Now, he is doing his PhD study in the Microelectronics Research Unit, Faculty of Information Technology and Electrical Engineering, University of Oulu, Finland. His research interests include gas sensors, photoelectric sensors, energy storage devices and perovskites.

Mikko Kokkonen received his bachelor's and master's degrees in Physics from the University of Oulu, Finland. He is currently a PhD student at the Microelectronics Research Unit of the Faculty of Information Technology & Electrical Engineering, University of Oulu, Finland. His current research focuses on the use of new materials as an RF lens. He is also interested in solar panels and green energy.

Parisa Talebi is a PhD student in Physics at the Nano and Molecular Systems Research Unit (NANOMO), University of Oulu, Finland, as a member of the Prof. Wei Cao group. Her research is on 'noble metal bridged ternary systems for promising clean and sustainable energy'. She obtained her MSc degree in Nano Physics at the University of Arak, Iran, under the supervision of Prof. Maziar Marandi. Her research interests include nanostructures, solar cells, photovoltaics, semiconductors, photocatalysts, hydrogen evolution, synchrotrons, and materials characterization.

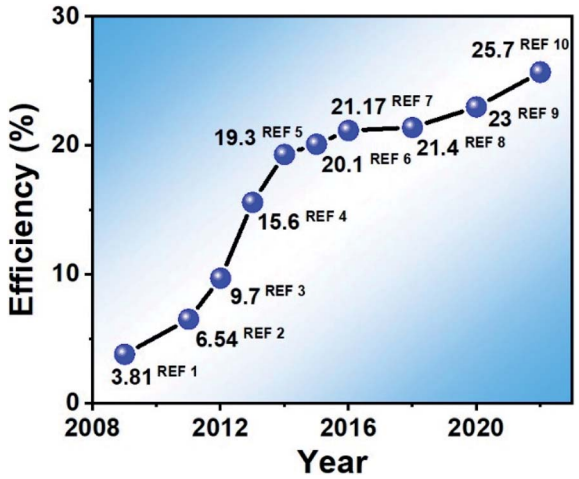

Fig. 1 Solar-to-electrical conversion efficiency evolution of lab-sized perovskite solar cells.

and advanced perovskite precursor inks for achieving efficient large-area PSCs and modules[29,30] while demonstrating striking stability when tested under both simulated and natural environmental conditions.[16–18] This report summarizes the trends that have emerged during the research and development of producing scalable perovskite precursor ink formulations, and it also discusses their contribution toward efficient, scalable, and durable PSC technology.

To begin with, the various types of scalable device designs are highlighted, along with a brief overview of their inherited advantages and limitations. Various device designs such as n-i-p, p-i-n, and hole transporting material (HTM)-free PSC configurations[27,31] are further discussed to establish the general understanding around scaling up approaches being applied on a variety of substrates to produce this low-cost and efficient solar cell technology.

Then, the historical evolution of testing various scalable precursor inks during the development of these configurations starting with lab-sized solar cell devices is presented. Numerous scalable coating schemes used to achieve large-area perovskite-based active layers are also discussed, providing insight into the abundant successes achieved in recent years to produce large-area PSMs. The evolution of state-of-the-art solar-to-electrical efficiencies for various large-area PSMs is also presented.

Various reports highlighting the robust photovoltaic performance of large-area perovskite solar modules in a variety of device configurations are also included in this review, providing a brief overview of the state-of-the-art of scalable precursor ink development in transforming the unstable lab-sized solar cells into large-area, robust, and low-cost solar cell technology. Hence, this review provides the latest insight into the technological research and development in producing novel and scalable precursor inks, as well as their successful integration in various device designs of PSC technology to create electricity and energize futuristic applications.

Jingshan Luo is a full professor and vice director of the Institute of Photoelectronic Thin Film Devices and Technology at Nankai University. He received his BSc degree from Jilin University in 2010 and his PhD degree from Nanyang Technological University in 2014. After that, he went to École Polytechnique Fédérale de Lausanne (EPFL) in Switzerland for post-doctoral research in the laboratory of Prof. Michael Grätzel, where he led the solar fuel subgroup. In 2018, he joined Nankai University. Jingshan Luo has authored/coauthored 1 book chapter and more than 100 peer-reviewed publications in Science, Nature Energy, Nature Catalysis and other journals in the field, which have garnered more than 20 000 literature citations and an h-index of 63 (Google Scholar). He has received many awards and honors, such as the MIT Technology Review Innovators under 35 China award and was named a Highly Cited Researcher (2018–2021) by Clarivate Analytics.

*Prof. Ana Flávia Nogueira obtained her bachelor's degree in Chemistry from the University of São Paulo (1996) and master's (1998) and PhD degrees in Chemistry from the University of Campinas (2001). She worked as a post-doctorate fellow at Imperial College, UK (2001–2002) and as a visiting researcher at Stanford University (2017–2018). At the moment, Ana Flavia is a Full Professor in the Chemistry Institute at UNICAMP and Director of the Center for Innovation on New Energies (CINE, **https://www.cine.org.br**). Prof. Nogueira's research focuses on the development of functional (nano)materials and their application in solar energy conversion. She has experience in the field of perovskite solar cells, perovskite quantum materials and dense energy carriers (generation of solar fuels through photoelectrocatalytic systems using water, CO_2 and other low added value substrates). She has published more than 170 papers, seven book chapters, one book and 3 patents. Her h-index is 40. The Laboratório de Nanotecnologia e Energia Solar (LNES) founded in 2005 has leadership in dye sensitized organic solar cells and perovskite solar research in Brazil and Latin America. In 2020 she was awarded the ACS Leadership in Academia Award.*

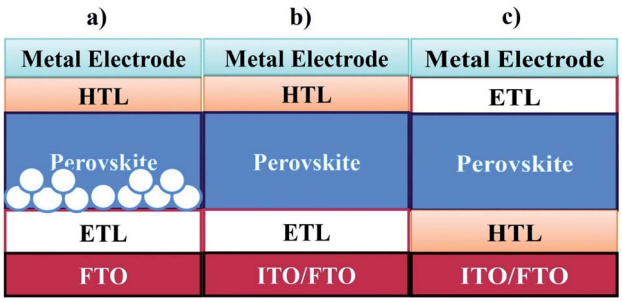

Fig. 2 Three fundamental and scalable configurations: (a) mesoporous n-i-p, (b) planar n-i-p, and (c) planar p-i-n, which have been reported for scaling-up during the emergence of perovskite solar cell technology in recent years (reproduced from ref. 31 with permission from the Royal Society of Chemistry).

2. Approaches for scaling-up various device designs of perovskite solar cell technology

The solution processing associated with individual layers of perovskite solar cells (PSCs) greatly influenced the scaling-up of technology from lab-sized devices to large-area modules, which have been fabricated on a variety of substrates.[32–38] In this regard, numerous configurations[39–42] initially designed to produce lab-sized PSC devices have also been explored to scale-up the technology.[43–46] Notably, three fundamental configurations (mesoporous n-i-p, planar n-i-p, and planar p-i-n) have emerged as the most applied in the scaling-up of PSCs (Fig. 2).

Motived by the solid-state dye-sensitized solar cell (ss-DSSC) configuration,[22,47,48] perovskite sensitized-based lab-sized solid-state solar cells were initially reported,[43,49–51] now known as the mesoporous n-i-p perovskite solar cell device design (Fig. 2a). In this structure, the TiO_2-based electron transporting layers (ETLs) are achieved by first fabricating the compact layer (~5–70 nm in thickness) either by spray pyrolysis,[52–56] spin coating[44,45,49,57,58] or atomic layer deposition (ALD)[59–63] on the desired substrates. After that, an additional mesoscopic layer of TiO_2-based ETL is fabricated either by spin coating or screen-printing[64–68] processes before depositing the perovskite-based light-absorbing layers, hole transporting layer (HTL), and metal contacts (Table 1).

Nevertheless, the mesoporous TiO_2 has been systematically removed from the mesoporous n-i-p device design, for the following reasons: (1) achieving low temperature and binder-free based ink or paste formulations of nanoparticles based on TiO_2 has remained challenging when attempting to achieve scalable mesoporous n-i-p-based configurations on flexible polymer substrates. (2) The additional step of fabricating

Trystan Watson is a Professor in Photovoltaics and Director at the SPECIFIC Innovation and Knowledge Centre. After completing an undergraduate Chemistry Degree and Engineering Doctorate in Steel Technology at Swansea University, Prof. Trystan moved to Corus Strip Products (now Tata Steel) as a product development engineer and a theme leader for the process technology group in the engineering doctorate scheme. In 2007, Prof. Trystan returned to academia to take up a research position in the development of dye-sensitized solar cells on metal substrates. Since then his research has focused on thin film printed PVs with a specialism in developing new technologies for the manufacture of solution processable photovoltaics such as perovskites and OPVs including deposition (roll-to-roll and sheet-to-sheet) and curing processes and their characterisation using electrochemistry, photochemistry and optoelectronic methods. He currently leads PV research at SPECIFIC and his research goal is to take new photovoltaic materials and develop the manufacturing pipeline for fabrication at scale. During his career, Prof. Trystan has published over 150 academic papers and is a chartered engineer with the IOM3 and a fellow of the Royal Society of Chemistry. Trystan is married with three daughters and a son and spends most of his home life wrapped around their fingers.

Syed Ghufran Hashmi is a Tenure Track Assistant Professor in Printed Electronics at the Microelectronics Research Unit of the University of Oulu, Finland. He has received numerous prestigious funds in the capacity of Project Leader and Principal Investigator from top funding organizations including Technology Industries of Finland Centennial Foundation, Jane and Aatos Erkko Foundation, Business Finland and Academy of Finland for the research and development of next-generation photovoltaic devices such as dye-sensitized solar cells and perovskite solar cells. He received his DSc degree in Engineering Physics from Aalto University – Finland in 2014. Before that, he received his MSc degree in Micro- and Nanotechnology from Helsinki University of Technology – Finland in 2009 and BS degree in Biomedical Engineering from Sir Syed University of Engineering and Technology – Pakistan in 2002. He has authored nearly 30 scientific publications, which have received 1120+ citations. His research interests include solar cells, printed electronics, energy harvesting, solar fuels, printable batteries and supercapacitors.

Table 1 Overview of the scalable perovskite solar cell device designs that have been reported in recent years

Deposition method										
Perovskite	ETL	HTL	Structure	Architecture	Contacts	Precursor ink	Area (active area cm^2)	PCE (%)	Substrate	Year	Ref.
Spin-coating	Spin-coating	Spin-coating	Modules p-i-n	p-i-n	LiF/Al	CH_3NH_3I and PbI_2 were stirred in a mixture of DMSO : GBL (3 : 7, v/v)	10 × 10 (60)	8.7% @ 1 sun	ITO-glass	2014	95
Spin-coating	Screen-printing	Spin-coating	Modules	Mesoporous n-i-p	Au	CH_3NH_3I and $PbCl_2$ (molar ratio 3 : 1) in DMF	5 × 5 (16.8)	5.1 @ 1 sun	FTO-glass	2014	96
Spin-coating	Spray pyrolysis	Spin coating	Modules 10 sub-units	p-i-n	Au	$MAPbI_3$ solution (40 wt%) was prepared by mixing the MAI powder and PbI_2 (1 : 1 mole ratio) in DMF	10 × 10 (40)	12.9 @ 1 sun	FTO-glass	2015	97
Slot-die coating	Slot-die coating	Slot-die coating	Modules	n-i-p	Ag	PbI_2 (322 mg mL^{-1} in DMF) and CH_3NH_3I (10 mg mL^{-1} in 2-propanol)	10 × 10 (40)	11.96 @ 1 sun	ITO-glass	2015	98
Dropping by micropipette	Screen-printing	—	Modules	n-i-p	C	The equimolar ratio of PbI_2 and CH_3HN_3I in γ-butyrolactone	10 × 10 (70)	10.74 @ 100 W white light LED light	FTO-glass	2016	99
Spray coating	Spray pyrolysis	Spin coating	Modules	n-i-p	Au	Mixed solution of DMF (dimethylformamide) : γ-butyrolactone (GBL) (v/v) to prepare the 0.8 M $MAPbI_{3-x}Cl_x$	10 × 10 (40)	15.5 @ 1 sun	FTO-glass	2016	100
Dipping PbI_2 substrates into MAI in IPA solution	Spray pyrolysis/ spin coating	Air assisted blade-coating	Modules	Mesoporous n-i-p	Au	PbI_2 substrates and MAI in IPA solution (10 mg mL^{-1})	10 × 10 (50)	12.6 @ 1 sun	FTO-glass	2017	101
Pressure processing	Spin coating	Spin coating	Single-cell	Mesoporous n-i-p	Au	$CH_3NH_3I{\cdot}3CH_3NH_2$ and $PbI_2{\cdot}CH_3NH_2$, in a molar ratio of 1 : 1; $CH_3NH_3I{\cdot}3CH_3NH_2$ and $PbI_2{\cdot}CH_3NH_2$ precursors were prepared by inducing CH_3NH_2 gas	8 × 8 (36.1)	12.1 @ 1 sun	FTO-glass	2017	102
Vapor–solid reaction method	Soaking and heating	Spin coating	Modules	n-i-p	Au	$Cs_xFA_{1-x}PbI_{3-y}Br_y$	8 × 8 (41)	12.24 @ 1 sun	FTO-glass	2018	50
Megasonic spray-coating	Thermal evaporation	Spin-coating	Single-cell	p-i-n	Cu	400 mg mL^{-1} PbI_2 in DMF/DMSO (volume ratio = 1 : 1) and MAI powder	7.5 × 7.5 (18)	16.9 @ 1 sun	ITO-glass	2018	57
Inkjet printing	Spin coating	Spin-coating	Single-cell	Mesoporous n-i-p	Au	$CH_3NH_3PbI_3$	~3.1 × 3.1 (2.02)	17.74 @ 1 sun	FTO coated substrate	2018	39
Spin coating	Spin coating	Spin coating	Single-cell	n-i-p	Ag	$[CsPbI_3]0.05[(FAPbI_3)0.85(MAPbBr_3)0.15]0.95$ in DMSO/DMF with a 5% molar ratio PbI_2 excess	14 × 14 (1.08/ 2 × 2 cell)	17.39 @ 1 sun	FTO-glass	2018	45

Table 1 (*Contd.*)

Deposition method											
Perovskite	ETL	HTL	Structure	Architecture	Contacts	Precursor ink	Area (active area cm^2)	PCE (%)	Substrate	Year	Ref.
Bar-coating	Bar-coating	Spin coating	Modules	n-i-p	Au	MAI and PbI_2 at an equimolar ratio were dissolved in mixed NMP : DMF (9 : 2)	8 × 10	17.28 @ 1 sun	ITO-glass	2019	103
Blade-coating	Spin coating	Spin coating	Single-cell	n-i-p	Au	461 mg of PbI_2, 78 mg of DMSO, and 159 mg of MAI dissolved in 600 mg of DMF and 0.05% ZnP	4 × 4	20.5 @ 1 sun	FTO-glass	2019	44
Air-knife-assisted D-bar coating	Spin coating	Spin coating	Single-cell	n-i-p	Au	0.12 mmol GAI, 1.78 mmol MAI, 0.7 mmol PbI_2 (10 mol% PbI_2 excess) and 0.4 mmol $PbAc_2$ were dissolved in 1 mL 2-ME	4.8 × 9.6 (16)	13.85 @ 1 sun	FTO-glass	2019	104
Solution-bathing	Spin coating	Spin coating	Single-cell	p-i-n	Au	PbI_2 (1.15 M), FAI (1.09 M), $PbBr_2$ (0.20 M), MABr (0.14 M) and CsI (0.06 M) in a mixed solvent of DMF/DMSO/NMP (DMF/DMSO, 4/1, v/v)	5 × 5 (1.00)	18 @ 1 sun	ITO-glass	2020	58
D-bar coating	Spin coating	Spin coating	Modules 10 sub-cells	n-i-p	Au	Dissolving 553.8 mg of the $FAPbI_3$ powder, 26.6 mg of CsBr, 45.8 mg of $PbBr_2$, and 20.4 mg of MACl in 700 μL DMF or HMPA; for the Lewis base additive, 0.6 mmol DMSO or 0.6 mmol HMPA was included in the precursor solution	5 × 5 (18.66)	17.01 @ 1 sun	FTO-glass	2020	43
Spin-assisted solvent extraction	Spin coating	Spin coating	Modules	n-i-p	Ag	An equal amount of MAI and PbI_2 (or FAI, MAI, and PbI_2 mixture or FAI, MAI, PbI_2, and $PbBr_2$ mixture) was dissolved in 2P to make a precursor solution with a concentration of 1.5 M	10 × 10 (25.2)	14.36 @ 1 sun	ITO-glass	2020	105
Slot-die coating	Slot-die coating	Slot-die coating	Single-cell/modules	p-i-n	Ag	276 mg PbI_2, 96 mg MAI, and 0.18 mg PEG were dissolved in the solvent mixtures of GBL and DMSO	2 × 2 (0.09; cut from 12 × 12)/4 × 4(3.78)	11 @ 1 sun/10.34 @ 1 sun	FTO-glass	2020	106

Table 1 (*Contd.*)

Deposition method											
Perovskite	ETL	HTL	Structure	Architecture	Contacts	Precursor ink	Area (active area cm^2)	PCE (%)	Substrate	Year	Ref.
HPNE strategy assisted slot-die coating	Chemical bath deposition	Spin coating	Modules	n-i-p	Au	$FA_{0.91}Cs_{0.09}PbI_3$ perovskite precursor was prepared in a mixed solvent (DMF : DMSO = 4.75 : 1) with a concentration of 1.25 M, 23 mol% MACl was added	0.6 × 3.4 × 5-sub-cell (10.2)	18.6 @ 1 sun	FTO-glass	2020	41
Slot-die method	Slot-die method	Slot-die method	Modules	n-i-p	Cr/Au	553.2 mg PbI_2 and 15.6 mg CsI were dissolved in 0.9 mL DMF and 0.1 mL DMSO; 75 mg FAI and 2.5 mg FACl were dissolved in 1 mL isopropanol	8 × 8 (35.80)	15.3% @ 1 sun	FTO-glass	2021	107
Spin-coating	Spin-coating	Spin-coating	Modules	n-i-p	Au	2.2 M PbI_2 and 28 mg CsI were dissolved in 1 mL DMF solution with different molar ratios of NH_4Cl (0, 0.1, 0.2, 0.3, 0.4, 0.5, 0.7 and 1.0 M)	10 × 10 (91.8)	10.25% @ 1 sun	ITO-glass	2021	108
Spin-coating	Chemical bath deposition	Thermal evaporation method	Modules	n-i-p	Au	1.35 M PbI_2 and 0.0675 M CsI were dissolved in a mixed solution (1.9 mL DMF and 0.1 mL DMSO); FAI 1000 mg; MAI 110 g; MABr 110 mg; MACl 110 mg, dissolved in 15 mL IPA	10 × 10 (91.8)	21.70% @ 1 sun	FTO-glass	2021	109
Spin-coating	Spin-coating	Spin-coating	Modules	n-i-p	Au	Lead iodide (1.51 M), formamidinium iodide (1.47 M), methylammonium bromide (0.03 M), lead bromide (0.03 M), and methylammonium chloride (0.6 M) in the mixed solvent of DMF : DMSO (8/1; v/v)	10 × 10 (45.6)	17.97% @ 1 sun	FTO-glass	2022	110

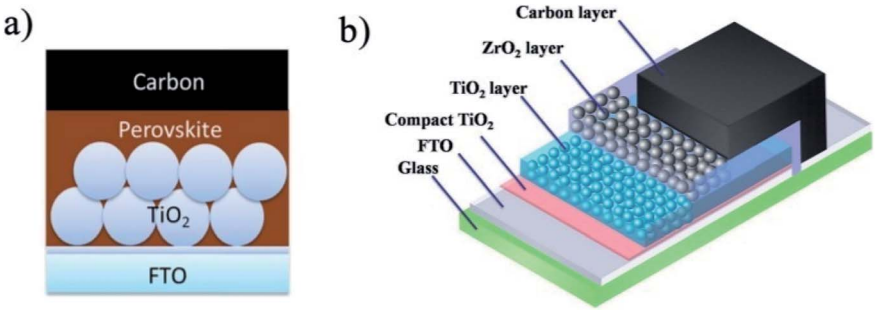

Fig. 3 Scalable carbon-based configurations. (a) Carbon-based perovskite solar cell (C-PSC) configuration (reproduced from ref. 93 with permission from the Royal Society of Chemistry). (b) C-PSC with a ZrO_2 spacer to keep the carbon layer separated from the photoanode (reproduced from ref. 94 with permission from the Royal Society of Chemistry).

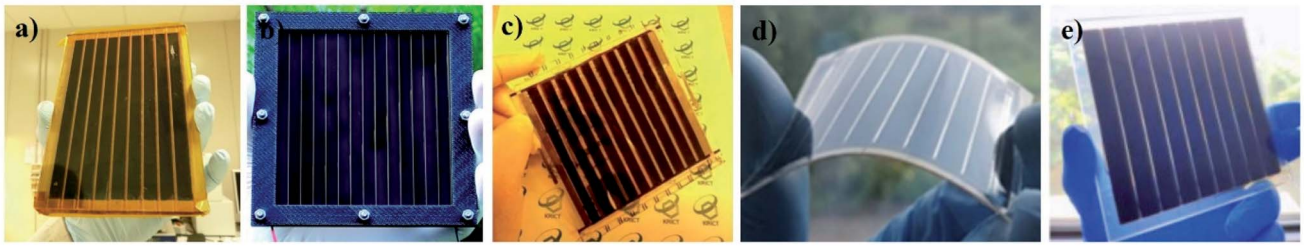

Fig. 4 Examples of various types of large-area perovskite solar modules fabricated on rigid and flexible substrates. (a) A mesoporous glass-based n-i-p solar module (reproduced from ref. 30 with permission from Elsevier, copyright 2022). (b) A planar n-i-p glass-based perovskite solar module (reproduced from ref. 111 with permission from the Royal Society of Chemistry). (c) An inverted p-i-n configured glass-based perovskite solar module (reproduced from ref. 95 with permission from the Royal Society of Chemistry). (d) An inverted p-i-n-based flexible solar module fabricated on PET polymer substrates (reproduced from ref. 112 with permission from the American Chemical Society). (e) A carbon-based triple-mesoscopic printable perovskite solar module on a rigid glass substrate (reproduced from ref. 66 with permission from Elsevier, copyright 2022).

a mesoporous TiO_2-based ETL in the device structure induces additional cost and time, which may limit the competitiveness of the technology compared to other existing solutions.

As a result, the n-i-p-based planar structure (Fig. 2b) gained attention since it can achieve good solar-to-electrical conversion efficiencies upon removing the mesoporous ETL layers from the traditional n-i-p device design of PSCs. Moreover, inspired by the solution processing of organic solar cells,[69–73] scaling-up schemes of PSC technology with a planar n-i-p device design have also been rapidly developed and demonstrated both on flexible polymers and rigid glass-based substrates.[32,41,45,46,74,75]

Similarly, the inverted structure of the p-i-n device design (Fig. 2c) has also been realized recently because of the availability of a wide range of material-based ink formulations already tested in lab-sized devices as well as in large-area module configurations, with impressive solar-to-electrical conversion efficiencies (Table 1).

In contrast to these traditional configurations, other scalable device designs *i.e.*, HTM- and metal contact-free carbon-based perovskite solar cell configurations (Fig. 3) have also been reported in recent years.[76–85] These novel device designs have emerged by first replacing the ruthenium dyes and liquid electrolytes from the monolithic DSSC configurations with a perovskite sensitizer.[86–88] This strategy allowed a low-cost, printable, and solid-state device configuration that demonstrated impressive solar-to-electrical energy conversion combined with exceptional stability when exposed to numerous simulated and natural climatic conditions.[1,89–92] Table 1 provides an overview of the scalable perovskite solar cells produced in various device designs. Fig. 4 represents the actual demonstrations of perovskite solar modules produced in some of the most established configurations discussed earlier in this section.

3. Historical evolution of perovskite precursors tested for scalable perovskite solar cells and modules

The solution processing associated with active layers of PSC technology, including perovskite-based light-absorbing layers, has greatly motivated research groups worldwide to create their novel and scalable precursor solutions that could be integrated into scalable cell architectures *via* various scalable material deposition methods, such as blade coating, inkjet printing, slot-die coating, or spraying-based material deposition technologies.

One of the initial studies was reported by Matteocci and co-workers, who demonstrated the first scalable and fully solid-state n-i-p-based perovskite solar modules (PSMs) fabricated on rigid glass substrates.[96] Interestingly, the spin-coating technique was chosen for the perovskite precursor ink deposition, comprising a mixed halide solution in *N*,*N*-dimethylformamide

Table 2 Large-area modules were fabricated in recent years by employing scalable perovskite precursor inks

Device structure	Perovskite precursor ink	Active area (cm^2)	PCE (%)	Year	Ref.
Glass/FTO/c-TiO_2/n-TiO_2/perovskite/P3HT/Au	Methylammonium iodide CH_3NH_3I and lead chloride $PbCl_2$ in *N*,*N*-dimethylformamide, molar ratio 3 : 1	16.8	5.1	2014	96
Glass/ITO/PEDOT : PSS/perovskite/PCBM/LiF/Al	The CH_3NH_3I and PbI_2 were stirred in a mixture of DMSO : γ-butyrolactone (GBL) (3 : 7, v/v) at 60 °C for 12 h	60	8.7	2014	95
Glass/FTO/BL-TiO_2/perovskite/Spiro-OMeTAD/Au	The 0.6 mL per sample of $CH_3NH_3PbI_{3-x}Cl_x$ perovskite precursor solution (40 wt%) was deposited by spin-coating at 2000 rpm for 60 s	10.08	13	2016	114
Glass/FTO/c-TiO_2/perovskite/Spiro-OMeTAD/Au	The typical recipe for 45 wt% precursor with 30% MACl additive is 0.2 g MAI, 0.580 g PbI_2, 0.025 g MACl, 0.524 g NMP and 0.429 g DMF	11.09	14.06	2017	115
PET/ITO/SnO_2/$Cs_{0.05}(FA_{0.85}MA_{0.15})_{0.95}Pb(I_{0.85}Br_{0.15})_3$/Spiro-OMeTAD-Au	Dissolving 1.3 M organic cations (0.85 FAI and 0.15 MABr) and a 1.4 M mixture of metal lead salts (0.85 PbI_2 and 0.15 $PbBr_2$) in a solvent of DMF/DMSO (4 : 1, by volume), and then a 34 μL CsI solution (pre-dissolved as a 2 M stock solution in DMSO) added	16.07	14.89	2018	116
Glass/FTO/c-TiO_2/mp-TiO_2/$MAPbI_{3-x}Cl_x$/Spiro-OMeTAD/Au	Different molar ratios of MACl/$HPbI_3$ are deposited on substrates. After thermal annealing, the obtained films react with CH_3NH_2 gas to form perovskite	12	15.3	2018	117
Glass/FTO/NiO/perovskite/DBL/G-PCBM/Ag	424 mg FAI, 1.136 mg PbI_2, 49 mg CH_3NH_3Br, and 160 mg $PbBr_2$ dissolved in 2.4 mL acetonitrile	36.1[a]	15.6	2019	118
PEN/ITO/np-SnO_2/porous-ZSO ETL/$(FAPbI_3)_{0.95}(MAPbBr_3)_{0.05}$/Spiro-OMeTAD/Au	1.26 mmol of PbI_2, 1.26 mmol of FAI, 0.06 mmol of $MAPbBr_3$, and 0.5 mmol of MACl in DMF/DMSO	90	15.5	2020	119
MgF_2/Willow glass/ITO/PTAA/MAPI-NH_4Cl/C_{60}/BCP/Cu	L-α-Phosphatidylcholine and methylammonium hypophosphite were added into ≈1.45 M $MAPbI_3$/2-ME solution at a concentration of ≈0.3 mg mL^{-1} and ≈0.15 vol%. 6×10^{-3} M NH_4Cl was added to the precursor	42.9	15.86	2020	120
Glass/FTO/ZnO–ZnS/mp-TiO_2/$CH_3NH_3PbI_3$/Spiro-OMeTAD/Au	1 mmol of MAI, 1 mmol of PbI_2, and MACl (<20 mol% of $MAPbI_3$) were dissolved in an 800 μL solution of CH_3NH_2 solution in ethanol, and 200 μL of CAN	12[a]	16	2020	121
PEN/hc-PEDOT : PSS/NiO_x/perovskite/PCBM/Ag	547 mg PbI_2, 46 mg $PbBr_2$, 150 mg FAI, 39 mg MAI and 0.02 wt% PU in 1.5 mL anhydrous DMF and 1.5 mL anhydrous DMSO	15	16.15	2021	113
Glass/FTO/c-TiO_2/mp-TiO_2/Perovskite/MW doped-PTAA/Au	$FAPbI_3$ (1.47 M) and $MAPbBr_3$ (0.18 M) precursor complexes in 1 mL of mixed DMF/DMSO solvent and 0.05 M CsI	42.8	17.05	2021	122
Glass/FTO/TiO_2/perovskite/$[M_4N]BF_4$/Spiro-OMeTAD/Ag	The $FA_{0.91}Cs_{0.09}PbI_3$ perovskite precursor was prepared in a mixed solvent (DMF : DMSO = 4.75 : 1) with a concentration of 1.25 M, 23 mol% MACl was added	7.92	19.0	2020	123
Glass/FTO/TIO_2/SnO_2/ink/BJ-GO/Spiro-OMeTAD/Cr/Au	645.4 mg PbI_2 and 18.2 mg CsI were dissolved in 0.9 mL DMF and 0.1 mL DMSO for the first deposited solution. 90 mg FAI and 4 mg FACl were dissolved in 1 mL isopropanol for the second solution	35.8	15.3	2021	107

[a] Aperture area.

(DMF) (Table 2) for the development of their 5 × 5 cm^2 PSM. The fabricated modules containing two types of HTMs exhibited similar (5.1%) solar-to-electrical energy conversion when tested under full sunlight illumination. Nevertheless, the modules fabricated with the traditional HTM (*i.e.*, Spiro-OMeTAD) exhibited higher long-term stability by maintaining more than 60% of their initial efficiency after 335 hours, compared to the alternative poly(3-hexylthiophene-2,5-diyl) (P3HT) polymer-based PSMs, in which the conversion efficiency was reduced by about 80% of the initial value after 170 hours.

This preliminary demonstration motivated research labs worldwide to further develop novel precursors that could be integrated into the desired scalable device configurations of PSC technology through established large-scale material deposition methods. For example, Xu and co-workers demonstrated a novel perovskite precursor ink that was introduced in triple mesoscopic carbon-based printable solar modules.[66] The novel precursor ink used in their study contained 5-ammonium valeric acid (5-AVAI) as a perovskite crystallization retarding agent, in addition to methylammonium iodide (MAI) and PbI_2, which were dissolved in γ-butyrolactone (GBL) solvent to attain the stable and compatible perovskite precursor ink formulation. As a result, successful fabrication of carbon-based PSMs was achieved by incorporating this novel precursor formulation through the slot-die coating technique over an aperture area of 80.55 cm^2. This resulted in achieving a striking conversion efficiency (12.87%) with an active area of 60.08 cm^2 when recorded under full sunlight illumination.

Contrary to the precursor inks demonstrated in the fabrication of rigid glass-based PSMs, other novel precursor inks have also been developed to produce large-area flexible perovskite solar cells and modules.[98,113] For example, Wang *et al.* recently reported a one-step perovskite precursor ink solution by dissolving PbI_2, $PbBr_2$, formamidinium iodide (FAI), MAI, and 0.02 wt% PU in 1.5 mL anhydrous DMF and 1.5 mL anhydrous dimethyl sulfoxide (DMSO) mixture solvent.[113] This novel precursor ink was meniscus-coated on the pre-HTL coated ITO-PET substrate to fabricate a large-area flexible solar module that exhibited impressive (>16%) solar-to-electrical energy conversion when tested under full sunlight illumination.

On the other hand, Castriotta and co-workers developed a blade-coated scalable precursor ink of the perovskite light-absorbing layer to produce a flexible perovskite solar module on an ITO-PET substrate.[112] A $Cs_{0.17}FA_{0.83}Pb(I_{0.9}Br_{0.1})_3$-based precursor ink was produced by dissolving CsI, $PbBr_2$, FAI, and PbI_2 in 1 mL of *N*-methyl-2-pyrrolidone (NMP)/DMF solvent, which was deposited on the HTL-coated ITO-PET substrate with N_2-assisted blade-coating, followed by heating (100 °C) for 45 minutes. With this inverted device design produced on an ITO-PET substrate, the flexible module also exhibited >10% power conversion efficiency (PCE) over a 15.7 cm^2 active area by exploiting blade deposition of the transporting layer and a stable double-cation perovskite (cesium and formamidinium, CsFA)-based light-absorbing layer. More impressively, outstanding light stability of the fabricated modules – over 1000 h, considering the recovery time (T_{80} = 730 h) – was also demonstrated, thus reinforcing the potential of this low-cost solution-based PV technology. Table 2 highlights some of the high-performing large-area modules that are being developed by incorporating scalable precursor inks of the perovskite-based light-absorbing layer.

4. Rheological characteristics of perovskite precursor inks and scalable coating methods for deposition of large-area perovskite precursors

Interestingly, the progressive transition not only induced innovativeness in scalable device designs, but also provided opportunities to develop advanced perovskite precursor inks *via* examining their rheological characteristics to facilitate the upscaling goals of PSC technology.

In this regard, various reports have frequently surfaced that highlight key rheological parameters (Fig. 5) such as contact angles, viscosity, density, surface tension, or boiling points of the fabricated perovskite precursor inks.[15,29,124–131] Such interesting trends led to the demonstration of various scalable device architectures of PSC technology fabricated by employing scalable perovskite-based precursor ink formulations along with scalable coating methods.

For example, Huang *et al.* reported the formulation of a novel PbI_2 ink by mixing traces of MAI and polyurethane (PU) as an additive with PbI_2 in the DMF/DMSO solvent mixture.[129] This novel ink engineering strategy regulated one of the key factors of rheological properties (*i.e.*, the viscosity) and influenced the chemical stability of the fabricated PbI_2 ink. As a result, both the successful room temperature-based scalable deposition of PbI_2 layers and the complete scalable deposition of perovskite light absorbing layers under ambient conditions were demonstrated through the two-step processing approach. An impressive 11.07% solar-to-electrical conversion efficiency was achieved for a 25 cm^2 based large-area perovskite solar module (PSM) when configured in a p-i-n based inverted configuration.

Fig. 5 Key rheological characteristics of high-performance perovskite precursor inks.

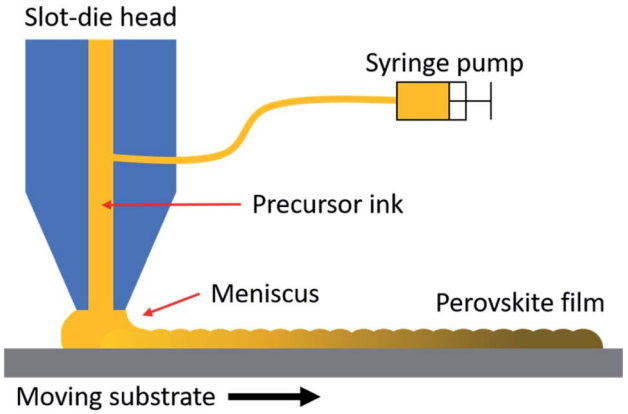

Fig. 6 Schematic illustration of the slot-die coating process.

In contrast, single-step processable inks have also been reported by incorporating starch as a 'rheological modifier',[126,127] which created a suitable viscosity for the fabricated perovskite inks to be deposited with a suitable thickness without increasing the concentration of perovskite precursors.[126] Roll-to-roll perovskite-based printed films and flexible solar cells have recently been demonstrated utilizing such inks, reaching a maximum power conversion efficiency close to 10% with required viscosities, with 50% less usage of the raw precursor materials along with a single processing step.[126]

Combined with advancements in similar rheological characteristics research, the rapid technological developments for material deposition schemes have also made it possible to achieve scalable layer formations of active layers for various next generation-based solar cell technologies.[132–134] This not only enables scalability of the energy systems but also achieves electrical, optical, dielectric, or optoelectronic properties of active layers with a reliable process control.[135–137]

In this regard, various scalable coating methods for large-area perovskite precursor deposition similar to other next generation-based PV technologies have also been explored to develop large area-based PSC technology on numerous substrates.[138–140] Some of these established scalable coating methods have been discussed in the following sub-sections.

4.1 Slot-die coating of perovskite precursor inks

Slot-die coating has remained one of the most popular schemes in fabricating flexible organic solar cells, as it allows the possibility for rapid coating and roll-to-roll fabrication of active layers on flexible substrates.[141–143] In this process, the slot-die head is placed close to the substrate and the ink is pumped into the head using a syringe. This creates a bridge of ink between the head and the substrate, which allows for a clean and rapid deposition of active layers on the desired substrates (Fig. 6).[141,144]

Vak *et al.* reported one of the first demonstrations of slot-die coating for producing a perovskite light-absorbing layer by modifying a 3D printer with a two-step processing approach.[145] First, the precursor ink of PbI_2 was coated on ZnO and dried to produce a PbI_2-coated ETL layer. Next, the substrate containing the active layers was dipped in the MAI solution to obtain the perovskite layer. Finally, the PSC assembly was completed by fabricating a P3HT-based hole transporting layer (HTL) and vacuum evaporating the silver (Ag) contact layer. The fabricated PSC exhibited an efficiency of 11.6%.

As a further advancement, large-area and roll-to-roll fabrication of glass and flexible perovskite solar cells, respectively, in a planar n-i-p configuration was demonstrated with slot-die printed active layers, except for the evaporated metal electrode.[98] In this work, the perovskite light-absorbing layer was also achieved with a two-step material deposition process, where the PbI_2 ink in DMF solvent was first slot-die coated on a ZnO-based ETL layer with various optimizations using gas quenching treatments. Next, the MAI solution was also coated with the same slot-die coating process to crystallize the perovskite light-absorbing layer. The HTL was achieved by coating with a P3HT solution followed by vacuum evaporation of the Ag contact layer. The fabricated devices on glass showed an efficiency of 11.96% on glass substrates. In contrast to rigid substrates, flexible perovskite solar cell modules were produced with roll-to-roll production on a 10 cm × 10 cm polymer substrate with five serially connected cells.

Demonstrations of single-step slot-die coatings are also reported wherein mixed cations,[146,147] additives,[148,149] and compatible solvents have been used to achieve homogeneous and large-area perovskite light-absorbing layers.[66,141] For example, Schmidt *et al.* reported a single-step slot-die processable coating of perovskite precursor ink that achieved 4.9% conversion efficiency on flexible ITO-PET substrates.[138] Slot-die coating of a novel precursor ink for triple mesoscopic printable perovskite solar modules was also recently demonstrated; a conversion efficiency of ~13% was obtained over an active area of 60.08 cm^2 when measured under full sunlight illumination intensity.[66]

These demonstrations suggest that single-step coating processes with slot-die coating might be more suitable for large-scale production of PSC technology. Reaching the desired result is made possible by forming a favorable combination of suitable

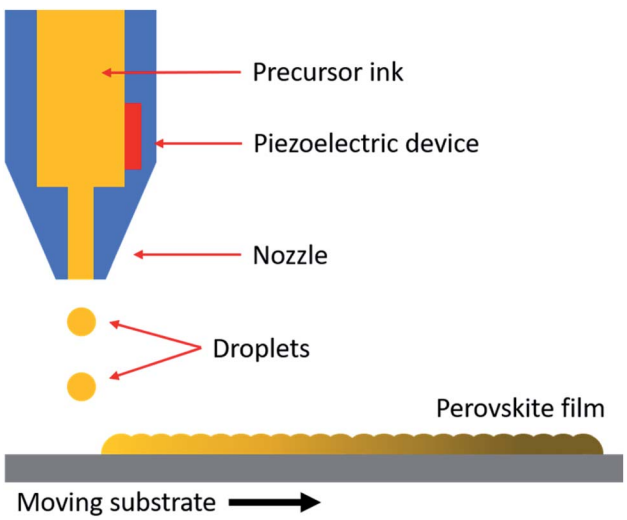

Fig. 7 Schematic illustration of the inkjet printing process.

precursor ink and substrate, along with the improved drying process of the precursor ink and its associated crystal growth.

4.2 Inkjet printing of perovskite precursor inks

The inkjet printing technique offers precise drop on demand (DOD)-based patterning for a variety of materials. In this method, the precursor ink remains stored in a nozzle, and pressure is created through a piezoelectric device to form the droplets. This allows for very precise control over the ink flow, which results in the smooth deposition of active materials over several types of substrates (Fig. 7).[150]

The scalability from lab-sized devices to large-area modules can be achieved by the rapid inkjet printing process, where individual layers like in slot-die coating can be printed directly on the desired substrates. Hashmi *et al.* demonstrated inkjet infiltration of a perovskite precursor ink on lab-sized PSCs and highlighted the performance reproducibility and reliable process control among the fabricated individual cells of the triple mesoscopic printable perovskite solar cells.[15] Similarly, Li *et al.* demonstrated inkjet printing of the perovskite precursor in the mesoporous n-i-p device configuration, where the perovskite precursor ink was deposited on TiO_2-based ETLs. The devices showed an efficiency of 12.3% in lab-sized PSC devices when measured under full sunlight intensity.[151]

Recently, Panasonic Corporation announced 16.09% solar-to-electrical energy conversion for a glass-based large-area perovskite solar module by using a coating method based on inkjet printing. In their module, every individual layer of the device design – including the perovskite layer – was deposited utilizing inkjet printing technology.[152] Another commercial player has also been developing large-area inkjet-printed flexible perovskite solar modules, which have started to become integrated into their commercial products.[153]

4.3 Blade-coating

Blade-coating is another potentially scalable deposition method that is widely used in various demonstrations of fabricating perovskite solar cells.[154–157] Fig. 8 illustrates the schematic of the blade-coating process, in which the precursor ink is dropped in front of a metallic or glass blade and then swept forward on a moving substrate to deposit a wet precursor layer.[158,159] The perovskite film thickness is determined by a few factors, including the meniscus of the solution that forms between the blade and substrate, the speed of the moving blade, the viscosity of the ink, and the concentration of the precursor ink.

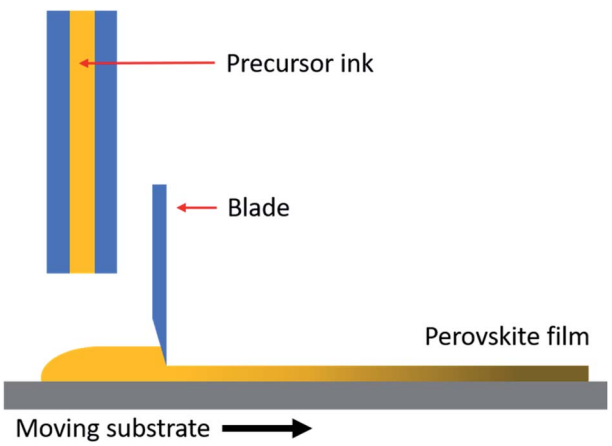

Fig. 8 Schematic illustration of the blade-coating process.

Similar to slot-die coating, both single- and two-step processing approaches can be applied to perovskite light-absorbing layer fabrication.[154,156] Gas and solvent quenching, and heating techniques have also remained popular schemes for controlling the crystallization and drying of the wet layers deposited through blade-coating from their respective precursor inks.[160,161]

Deng *et al.* performed single-step blade-coating of a perovskite precursor ink on glass substrates, by which 12.8% and 15.1% solar-to-electrical conversion efficiencies were achieved with two different HTM layers.[139] The fabricated ink was obtained by dissolving MAI and PbI_2 (1 : 1 molar ratio) in DMF, which was then coated with a glass blade on two different HTM (PEDOT : PSS and c-OTPD : TPACA) layers to fabricate and compare the inverted p-i-n configuration. A large grain-sized crystal-based perovskite layer was achieved with the demonstrated blade-coating method, which was effective over a long carrier diffusion length and led to high conversion efficiencies when tested under simulated full sunlight illumination.

In another study, Tang *et al.* applied a novel approach of mixing cesium (Cs^+) and bromine (Br^-) ions into the perovskite precursor solution, which also reduced the required film formation temperature.[135] Pinhole-free perovskite thin films with micrometer-sized grains have been obtained with the assistance of secondary grain growth with methylammonium chloride added into the precursor solution. The fabricated PSCs using such bladed perovskite layer attained an impressive 19.0% solar-to-electrical energy conversion; the best-stabilized conversion efficiency reached 19.3%.[135] Zhang *et al.* reported an impressive demonstration of an n-i-p design with two-step sequential blade-coating of high-quality perovskite layers for producing efficient solar cells and modules.[162] Their fabrication scheme involved the production of a SnO_2-based compact layer, achieved with a chemical bath process. Next, the sequential blade-coating steps were performed: DMF containing PbI_2-based precursor ink was first bladed over the compact layer and heated to achieve PbI_2 films. Then the mixed solution of FAI, methylammonium bromide (MABr), and methylammonium chloride (MACl) in isopropanol (IPA) was sequentially bladed over the PbI_2 layers, followed by an annealing step at 150 °C for perovskite crystallization. The fabricated solar cells with this two-step blade-coated processing yielded a conversion efficiency as high as >20% among lab-sized solar cells, whereas the large-area (5 cm × 5 cm and 10 cm × 10 cm) modules exhibited 16.54% and 13.32% conversion efficiencies, respectively.

4.4 Spraying

Similar to the previously discussed scalable fabrication schemes, spraying has also been widely used for precursor ink deposition to achieve large-area perovskite layers but also, deposition of other

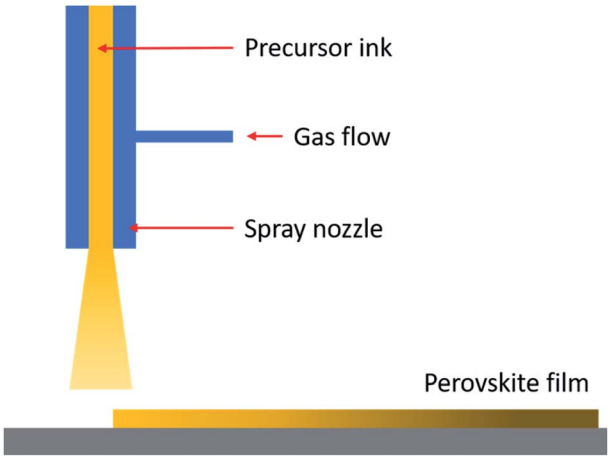

Fig. 9 Schematic illustration of the spraying process.

transporting layers.[100,163] This solution-based deposition scheme typically utilizes an ultrasonic tip vibrator to create a solvent mist or ink droplets that are directed to the substrate.[163] To do this, N_2 or O_2 can be used as a carrier gas to produce wet films on the desired substrates (Fig. 9).

Barrows *et al.* coated perovskite layers with a single step by spraying mixed solutions of MAI and $PbCl_2$ in DMF and DMSO solvents over PEDOT : PSS, and achieved 11% solar-to-electrical conversion efficiency in the inverted p-i-n configuration for lab-sized PSCs.[164]

Boopathi *et al.* controlled the volume of MAI through airbrush spraying followed by the deposition of PbI_2 through spin-coating to attain a uniform, stoichiometric and continuous perovskite film.[165] Their experiments showed that either a deficiency or surplus in the volume of MAI generates poor crystallinity and morphology, which gradually reduces device performance.[165] A power conversion efficiency (PCE) of 11.66% was reported when 300 μL of MAI solution was sprayed on 100 nm coated PbI_2 films. With data from 50 devices, the researchers demonstrated 10–11% solar-to-electrical conversion efficiencies under full sunlight illumination testing conditions. The inverted p-i-n device architecture of Ramesh *et al.* achieved an average power conversion efficiency of >9% using a single-step processed lead halide precursor ink that was similarly deposited through the spray-coating technique.[166]

From the perspective of scaling up, Tait *et al.* reported a perovskite PV module with a conversion efficiency of 11.7% with a 3.8 cm^2 aperture area using pinhole-free perovskite layers generated with ultrasonic spray-coating.[167] Similarly, fully spray-coated and scalable PSCs have also been reported with triple cation-based precursor ink formulation. These precursor inks have successfully been sprayed and converted into efficient light-absorbing perovskite layers, along with other sprayed active layers for producing high-performance and large-area PSCs.[168] This also offers the possibility for testing other novel multi-cation-based precursor inks that have been demonstrated for producing high-performance and lab-sized solar cells based on the spin-coating fabrication of perovskite light-absorbing layers.[169,170]

4.5 Other emerging scalable techniques for perovskite precursor deposition

In addition to the abovementioned scalable coating schemes, other interesting approaches have also been reported to produce both scalable and roll-to-roll coating-based rigid and flexible PSCs and modules. One such pioneer technique is gravure printing of active layers, which allows continuous and precise pattern printing on flexible polymer substrates. Kim and co-workers reported a successful fabrication scheme to produce an SnO_2-based ETL, perovskite layer, and Spiro-OMeTAD or poly(3-hexyl thiophene) (P3HT)-based HTL layers using gravure printing on flexible polymer substrates.[171] Interestingly, instead of single-step processing, the perovskite layer was fabricated in two steps. The PbI_2 coating was first performed by formulating a precursor ink in DMSO using a custom-built pilot-scale R2R printing machine. The coated PbI_2 roll was then divided into individual sheets, which were dipped in an MAI bath for perovskite layer formation and annealed at 100 °C for 10 minutes. Conversion efficiency of up to 17.2% was achieved for these flexible PSCs with a gravure printed HTM and thermally evaporated Ag contact electrode, over an active area of 0.052 cm^2.[171]

In addition to the gravure printing scheme, Hilt *et al.* recently reported a striking rapid spray plasma processing (RSPP) scheme for large-area perovskite layer deposition.[137,172] In their preliminary method, a novel perovskite precursor ink was deposited using standard spraying in ambient air using an ultrasonic atomizing nozzle.[172] The coated layer was immediately exposed to atmospheric pressure plasma to achieve rapid perovskite crystallization without post-processing steps. This rapid perovskite active layer formation offers the possibility to realize extremely fast inline production.[172] Rolston *et al.* further developed the technique and demonstrated >15% based perovskite modules at production speeds of >10 m min^{-1}, with perovskite active layer deposition at linear speeds of 12 m min^{-1}.[137]

Overall, the impressive progress in research being made with the abovementioned scalable fabrication processes suggests that a variety of precursor ink processing options are available, not only for perovskite layers but also for depositing other active layers of popular device designs of PSC technology. Results indicate that high performance and rapid production of futuristic perovskite solar modules is within reach, hence there is potential to compete with the existing (and currently dominant) Si-based PV systems. Table 3 summarizes several scalable coating methods for scalable perovskite layer deposition that are currently being used to produce large-area solar modules on a variety of substrates.

5. Evolution of stability of large-area perovskite solar modules with stable perovskite precursor inks

Like other existing next-generation-based photovoltaic technologies, one of the bottlenecks for the awaited commercial success of PSC technology is related to the long-term

Table 3 Recently reported large-area perovskite solar modules were produced by using scalable perovskite precursor inks along with various scalable coating techniques

Device structure	Perovskite ink composition	Coating method	Active area (cm^2)	PCE (%)	Ref.
Glass/ITO/PEDOT : PSS/perovskite/C_{60}/$PC_{61}BM$	MAI and $PbCl_2$ (3 : 1 molar ratio) in DMF	Slot-die	10	8.3	146
Glass/FTO/mp-TiO_2/ZrO_2/carbon/perovskite	MAI and PbI_2 in GBL with 5-AVAI additive	Slot-die	60.08	12.9	66
Glass/ITO/c-TiO_2/perovskite/Spiro-OMeTAD	MAI, $PbCl_2$, and Pb $(CH_3COO)\cdot 3H_2O$ in DMF	Slot-die	168.75	11.8	173
PET/ITO/SnO_2–KOH/perovskite/Spiro-OMeTAD/Au	FAI, MABr, PbI_2, and $PbBr_2$ in DMF and DMSO	Slot-die	16.07	15	116
Glass/FTO/c-TiO_2/perovskite/Spiro-OMeTAD	MAI and PbI_2 in DMF and DMSO	Inkjet	2	17.7	39
Glass/FTO/TiO_2/perovskite/Spiro-OMeTAD	MAI and PbI_2 in DMSO : GBL	Inkjet	4	13.2	174
Not reported	Not reported	Inkjet	802	16.1	152
Glass/FTO/SnO_2/perovskite/Spiro-OMeTAD	$MAPbI_3$ with $PbCl_2$ and $Pb(CH_3CO_2)_2\cdot 3H_2O$ in DMF	Blade	16.16	11.0	175
Glass/ITO/PTAA/perovskite/C_{60}/BCP	$MAPbI_3$ in DFM mixed with LP in DMF	Blade	33.0–57.2	15.3–14.6	29
Glass/FTO/SnO_2/perovskite/ Spiro-OMeTAD	FAI, MABr, PbI_2, and $PbBr_2$ in DMF : DMSO (4 : 1 volume ratio)	Blade	100	13.3	162
PET/ITO/PEDOT : EVA/ perovskite/PCBM : BCP	PbI_2, $PbBr_2$, $HC(NH_2)_2I$ and CH_3NH_3I in DMF : DMSO	Blade	36	17.2	176
Willow glass/ITO/PTAA/ perovskite/C_{60}/BCP/Cu	$MAPbI_3$ in 2-ME	Blade	42.9	15.86	120
Glass/ITO/TiO_2/perovskite/Spiro-OMeTAD	$PbCl_2$: MAI and $PbAc_2$: MAI in DMF	Spraying	3.8	11.7	167
Glass/FTO/TiO_2/perovskite/PTAA	MAI and $PbCl_2$ in IPA	Spraying	40	15.5	100
Glass/FTO/c-TiO_2/mTiO_2 + G/perovskite/Spiro-OMeTAD	FAI, PbI_2, MABr, $PbBr_2$, and CsI in DMF/DMSO	Spraying	108–82	13.4–15.3	140
Glass/ITO/NiO/$Cs_{0.17}FA_{0.83}PbI_3$/C_{60}	MAI, CsI and PbI_2 in DMF : DMSO (1 : 2 volume ratio)	RSPP	5.9	15.2	137
Glass/FTO/TiO_2/ZrO_2/carbon/perovskite	MAI and PbI_2 in GVL and MeOH	RbM	220	9	177

photovoltaic performance stability.[178–180] In this regard, inherent material-based degradation,[118,181] composition of precursor inks, effective perovskite layer crystallization, unique device designs, and effective sealing strategies significantly influence the overall stability of the fabricated PSCs and large-area modules against simulated and natural climatic conditions.[12,182]

Bu *et al.* used a scalable mixed cation ink of perovskite precursor to produce a large-area flexible perovskite solar module (PSM), which was deposited on an Alfa-SnO_2 compact layer-based flexible PET polymer foil *via* the spin-coating technique.[183] This scalable ink was formulated by dissolving 1.3 M organic cations (0.85 FAI and 0.15 MABr) and 1.4 M mixed lead salts (0.85 PbI_2 and 0.15 $PbBr_2$) in a solvent of DMF/DMSO (4 : 1, by volume). Next, 34 μL of CsI solution (pre-dissolved as a 2 M stock solution in DMSO) was added to achieve the desired $Cs_{0.05}(FA_{0.85}MA_{0.15})_{0.95}Pb(I_{0.85}Br_{0.15})_3$ perovskite precursor solution. The flexible large-area (5 cm × 6 cm) module exhibited impressive (>15%) solar-to-electrical conversion efficiency over an active area of 16.07 cm^2 when measured under full sunlight intensity conditions. Moreover, the fabricated flexible module also retained 80% of its original efficiency without encapsulation after 1000 h in dark storage combined with ambient air at ~20% relative humidity (RH) conditions.[183]

Nia and co-workers recently demonstrated >17% solar-to-electrical conversion energy based on a large-area PSM on a glass substrate with an active area of 42.8 cm^2.[184] The perovskite precursor ink to be coated on the large area was prepared by mixing $FAPbI_3$ (1.47 M) and $MAPbBr_3$ (0.18 M) complexes in 1 mL of mixed DMF/DMSO solvent. Next, 0.05 M CsI solution was added to the mixed solution to complete the recipe, in which the stock solution of CsI was made by dissolving 389.71 mg of CsI powder in 1 mL DMSO. The fabricated ink was deposited on a TiO_2-based ETL to produce a PSM with an n-i-p configuration. In combination with a poly(triarylamine) (PTAA)-based HTL, the fabricated modules showed not only higher solar-to-electrical energy conversion efficiency, but also exhibited impressive stability *via* maintaining >90% of the initial efficiency after 800 h of thermal stress at 85 °C.

In addition to the large-area modules based on conventional n-i-p and p-i-n configurations, other configurations such as the hole conductor-free carbon-based triple mesoscopic printable perovskite solar cells (CPSCs)[185,186] have also been recognized as potential low-cost configurations, with a proven record of exhibiting high stability when tested under various natural and simulated environmental conditions.[12,187] The promising demonstrations of scalability and stability reported with this unique device design can be explained by several factors such as (1) the hydrophobic nature of the carbon electrode, which effectively suppresses moisture penetration in the device structure,[18] (2) effective sealing procedures for retarding the rate of degradation,[12,187] and (3) the novel perovskite precursor ink, which has been introduced with scalable fabrication schemes such as inkjet printing[15,188] or slot-die coating[66] methods. As a result, this low-cost device design of the PSC ensures scalability with reliable process control for the successful deployment of this low-cost PV technology.[15,189]

In addition to research labs, several companies have also recently built or announced the production of large-area perovskite modules.[190–192] This indicates the relevance and

Table 4 Recently reported stable large-area perovskite solar modules with scalable precursor ink compositions of perovskite light harvesters

Device structure	Perovskite precursor ink	Method of deposition	Active area (cm^2)	Efficiency (%)	Stability	Ref.
Glass/FTO/SnO_2/carbon/perovskite/PEABr/PMMA/Spiro-MeOTAD/Au	The perovskite solution of $Cs_{0.05}FA_{0.8}MA_{0.15}PbI_{2.5}Br_{0.5}$ for the conventional planar structure was obtained by dissolving CsI, FAI, MAI, PbI_2, and $PbBr_2$ in DMF and DMSO and stirring the solution at 60 °C for 3 h. The DMSO/DMF ratio was 1 : 4	Drop-casting	4.32	8.7	Retains more than 92% of its initial performance after 3000 h of damp-heat aging at 85 °C/85% relative humidity	195
Glass/FTO/ETL/perovskite/$[M_4N]BF_4$/HTL/Au	The $FA_{0.91}Cs_{0.09}PbI_3$ perovskite precursor ink was prepared in mixed solvents (DMF : DMSO = 4.75 : 1) with a concentration of 1.25 M, 23 mol% MACl was added	Slot-die coating	7.92	19.6	Maintained over 80% of its initial efficiency after 551 h at 25 °C, humidity < 20%	41
Glass/FTO/TiO_2/perovskite/Spiro-OMeTAD	FAI (1 M), PbI_2 (1.1 M), MABr (0.2 M), $PbBr_2$ (0.22 M) and CsI (0.05 M) in DMSO and DMF (1 : 4 v/v)	Spin-coating	8.1	12.7	Retains 85% of its initial PCE after 400 h with an AM 1.5G Oriel solar simulator at an illumination intensity of 100 mW cm^{-2}	196
Glass/FTO/c-TiO_2/perovskite/Spiro-OMeTAD/Ag	A 30 wt% and 45 wt% equimolar ratio MAI and PbI_2 precursors with different amounts of MACl additive (15%, 30%, 50%, 70%, and 100% molar ratios) in a mixed solvent (NMP/DMF 9/8 volume ratio) were used. The typical recipe for 45 wt% precursor with 30% MACl additive is 0.2 g MAI, 0.580 g PbI_2, 0.025 g MACl, 0.524 g NMP and 0.429 g DMF	Blade-coating	11.09	17.33 ± 0.28	Retains 80% of its initial efficiency after 3000 h measured in air at AM 1.5G and illumination at 100 mW cm^{-2}	197
Glass/FTO/bl-TiO_2/n-TiO_2/perovskite/Spiro-OMeTAD/Au	$(HC(NH_2)_2PbI_3)_{0.85}(CH_3NH_3PbBr_3)_{0.15}$ prepared from mixing $HC(NH_2)_2PbI_3$ and $CH_3NH_3Br_3$ in DMF and DMSO with the corresponding volume ratio	Spin-coating	16	12.1	Remains stable after 2 months of storage under ambient conditions	198
PET/ITO/SnO_2/perovskite/SpiroOMeTAD/Au	1.3 M organic cations (0.85 FAI and 0.15 MABr) and 1.4 M mixture of metal lead salts (0.85 PbI_2 and 0.15 $PbBr_2$) in a mixture solvent of DMF/DMSO (4 : 1, by volume), and then a 34 μL CsI solution (pre-dissolved as a 2 M stock solution in DMSO) was added to achieve the desired $Cs_{0.05}(FA_{0.85}MA_{0.15})_{0.95}Pb(I_{0.85}Br_{0.15})_3$ perovskite precursor solution with excess lead halide	Slot-die coating	16.07	14.47	Retains 80% of its initial efficiency after 1000 h dark storage in ambient air (~20% RH) without encapsulation	183
Glass/ITO/PEDOT : PSS/$MAPbI_3$/C_{60}/BCP/Ag	An equal amount of MAI and PbI_2 was dissolved in 2P to make a precursor solution with a concentration of 1.5 M	Spin-coating	25.2	14.36	63% of the efficiency was left when the cell was exposed to air with a relative humidity of 30–50% for 1 month	199
Glass/FTO/c-TiO_2/m-TiO_2/perovskite/Spiro-MeOTAD/Au	$H_3NH_3I \cdot 3CH_3NH_2$ and $PbI_2 \cdot CH_3NH_2$, in a molar ratio of 1 : 1; $CH_3NH_3I \cdot 3CH_3NH_2$	Spin-coating	27.5	12.1	Maintained over 90% of its initial efficiency after 500 h; pressure, temperature, and peeling speed were 120 bar (thickness of 400 nm), 50 °C, and 50 mm s^{-1} respectively	200
Glass/ITO/PTAA/perovskite/C_{60}/BCP/Cu	1 M $MAPbI_3$ in DMF	Blade-coating	30.82	15.3	PCE is maintained over 20 days of storage in the dark in a N_2 atmosphere	201

Table 4 (*Contd.*)

Device structure	Perovskite precursor ink	Method of deposition	Active area (cm^2)	Efficiency (%)	Stability	Ref.
Glass/FTO/c-TiO_2/me-TiO_2/perovskite/Spiro-OMeTAD/Au	$CH_3NH_3I \cdot 3CH_3NH_2$ and $PbI_2 \cdot CH_3NH_2$, in a molar ratio of 1 : 1	Pressure processing	36	15.7 (12.1 certified)	Kept 90% of its initial efficiency after continuous working at the maximum power point under light for 500 h	200
Glass/FTO/SnO_2/perovskite/Spiro-MeOTAD/Au	The CsBr film deposition rate was maintained at 0.3 Å s^{-1}. After the crucible cooled down, the PbI_2 films were deposited successively at a rate of 3 Å s^{-1}. Then, the as-prepared composite films were transferred into a tube furnace facing another glass substrate with FAI/FACl film sprayed on it	Spin-coating	41.25	17.29	Maintained 83% of its initial efficiency after 200 h under ambient conditions (RH = ~30%, 25 °C)	50
Glass/FTO/cTiO_2/mTiO_2/perovskite/Spiro-OMeTAD/Au	PbI_2 substrates and MAI in IPA solution (10 mg mL^{-1})	Vapor–solid reaction method	50.6	12.6	Retaining ~91% of the initial PCE value after 1630 h of an endurance test under dark and dry conditions (relative humidity < 30%)	140
Glass/FTO/TiO_2/ZrO_2/carbon/perovskite (drop cast perovskite through the carbon layer)	PbI_2 and CH_3HN_3I, in a molar ratio of 1 : 1, in γ-butyrolactone	Blade-coating	70	10.74	Maintained over 95% of its initial efficiency after 2000 h under ambient conditions (temperature ≈ 25 °C, and humidity ≈ 65% RH)	99
Glass/ITO/SnO_2/perovskite/Spiro-OMeTAD/Au	A mixed organic cation solution (FAI 592 mg, MAI 296 mg, MABr 74 mg, MACl 74 mg, dissolved in 10 mL isopropanol) was spin-coated at 3000 rpm for 30 s	Spin-coating	91.8	10.25	Kept 90% of the initial efficiency for more than 450 h	108
Glass/FTO/cTiO_2/mTiO_2/mZrO_2/m-carbon/perovskite	An equimolar solution of PbI_2 and MAI in γ-butyrolactone	Screen-printing	198	3–5	Maintained its performance for over 288 h at 70% RH. It was then stored in a box with silica (≈30% RH) and tested infrequently. After 528 h following fabrication, it had reached almost 5% PCE, 19.6 V V_{OC} (0.891 V per cell), 125 mA I_{SC} (13.9 mA cm^{-2}), and 40% FF	202
Glass/FTO/TIO_2 perovskite/NBP/MoO_3/Au	—	Vacuum deposition	400	21.3	The efficiency increased by 1% from the original value in the air at a humidity of 35% for 189 days	203

importance of producing efficient and large-area PSMs on a variety of substrates through intelligent designing of novel configurations,[191,192] along with the development of novel and scalable precursor inks[193,194] that can contribute to the continuous improvements in solar-to-electrical energy conversion and show impressive stability when tested under harsh environmental conditions. Table 4 summarizes the descriptions of large-area stable PSMs reported in recent years with various scalable perovskite precursor ink formulations.

6. Summary and conclusions

The emergence of solution-processed perovskite light harvester-based photovoltaic technology has shown potential for efficient and bulk electricity generation, which may aid in the response to the growing global energy demand. The versatility and use of low-cost, easily available materials offer great flexibility in designing a wide variety of configurations that can be fabricated on numerous substrates, such as flexible polymers or rigid glass, according to the targeted applications.

The intense research and development activities that have progressed in recent years have provided the necessary understanding for transforming these materials into solution-processable inks or paste that can produce this technology with established and scalable coating or printing methods, which may impact production costs. In addition, these scalable production schemes also provide opportunities to scale up technology on both rigid and flexible substrates with a reliable process control that significantly influences the commercial success of nanotechnology-based electronics or advanced energy systems.

Overall, fabricating novel and advanced perovskite precursor inks to support the scaling up of PSC technology has remained one of the key focus areas in the past decade, due to the potential to achieve efficient, scalable, and stable device configurations of this solution-processed and low-cost PV technology. Fabricating such advanced precursor inks with tunable characteristics consequently provides notable flexibility for the various established and scalable coating methods discussed in this review.

Interestingly, although advanced research trends have emerged for examining key rheological characteristics, which led to developing a variety of scalable perovskite precursor inks, their deposition through blade coating or slot die coating schemes appear to be the most predominant method for producing scalable PSCs.[162,173,201,204] This is understandable, since the post-processing methods such as selective laser scribing, followed by large-area coatings of active layers including the perovskite-based light absorbing layer by these schemes have been proposed to facilitate the production of established serially connected modules.[205–207]

In contrast, other potential scalable methods such as drop-on-demand inkjet printing[136,208–210] have yet to be proven as a reliable process step for large perovskite layer deposition in order to overcome advanced key challenges related to creating flexibility in pattern designs of any choice through high precision and resolution.[15,17,211] These challenges call for the development of room temperature-based chemically stable precursor inks that can pass through without clotting the micro-nozzles of the inkjet cartridges, in order to deliver precise microlitre-sized drop volumes over the desired surfaces.[15,17]

In this regard, some interesting guidelines may be taken from a few novel additives[126,127] discussed earlier in this work for developing desired stable perovskite precursor inks to be used with inkjet printing technology. These additives were claimed to influence the chemical stability of the formulated inks when used with blade coating or gravure printing-based material deposition methods. Thus, use of such novel additives might also aid in developing chemically stable perovskite ink formulations to be used in inkjet technology for achieving high resolutions based on versatile pattern designs.

Alternatively, other grand challenges such as the development of eco-friendly perovskite precursor inks have also been realized to promote the global green energy transition, which presently is bottlenecked when using classical Pb-based precursor inks. Therefore, interesting progress in this growing area of ecologically friendly precursor ink development may also be anticipated, which could provide new opportunities for the safe integration of this low-cost and efficient PV technology.

Author contributions

Ethan Berger, Mohammad Bagheri, Somayyeh Asgari, Jin Zhou, Mikko Kokkonen and Parisa Talebi contributed to manuscript planning and communication, compiling sections with writing, drafting figures and tables, reference management and commenting on the final version of the manuscript. Jingshan Luo, Ana Flávia Nogueira and Trystan Watson contributed with an overview and comments on the manuscript. Syed Ghufran Hashmi supervised the research work and contributed with funding acquisition, outline drafting, reviewing, and editing the text, tables, and illustrations of the manuscript.

Conflicts of interest

There are no conflicts to declare.

Acknowledgements

The course funding (Perovskite based Photovoltaics) from UniOGS is acknowledged. Syed Ghufran Hashmi is grateful to the Jane and Aatos Erkko Foundation and Technology Industries of Finland for CAPRINT project funding (Decision# 2430354811). Mikko Kokkonen is grateful to the Academy of Finland 6Genesis Flagship (grant no. 318927). Jingshan Luo acknowledges the funding support from the 111 Project (grant no. B16027). Ana Flávia Nogueira gratefully acknowledges support from FAPESP (São Paulo Research Foundation, Grant Number 2017/11986-5), Shell and the strategic importance of the support given by ANP (Brazil's National Oil. Natural Gas and Biofuels Agency) through the R&D levy regulation. Thank you to EPSRC for funding the SPECIFIC Innovation and Knowledge Centre and ATIP Programme Grant (EP/N020863/1, EP/T028513/1).

References

1 A. Kojima, K. Teshima, Y. Shirai and T. Miyasaka, *J. Am. Chem. Soc.*, 2009, **131**, 6050–6051.
2 J.-H. Im, C.-R. Lee, J.-W. Lee, S.-W. Park and N.-G. Park, *Nanoscale*, 2011, **3**, 4088–4093.
3 H.-S. Kim, C.-R. Lee, J.-H. Im, K.-B. Lee, T. Moehl, A. Marchioro, S.-J. Moon, R. Humphry-Baker, J.-H. Yum, J. E. Moser, M. Grätzel and N.-G. Park, *Sci. Rep.*, 2012, **2**, 591.
4 J. T.-W. Wang, J. M. Ball, E. M. Barea, A. Abate, J. A. Alexander-Webber, J. Huang, M. Saliba, I. Mora-Sero, J. Bisquert, H. J. Snaith and R. J. Nicholas, *Nano Lett.*, 2014, **14**, 724–730.
5 H. Zhou, Q. Chen, G. Li, S. Luo, T.-b. Song, H.-S. Duan, Z. Hong, J. You, Y. Liu and Y. Yang, *Science*, 2014, **345**, 542–546.
6 W. S. Yang, J. H. Noh, N. J. Jeon, Y. C. Kim, S. Ryu, J. Seo and S. I. Seok, *Science*, 2015, **348**, 1234–1237.
7 M. Saliba, T. Matsui, J.-Y. Seo, K. Domanski, J.-P. Correa-Baena, M. K. Nazeeruddin, S. M. Zakeeruddin, W. Tress, A. Abate, A. Hagfeldt and M. Grätzel, *Energy Environ. Sci.*, 2016, **9**, 1989–1997.
8 M. M. Tavakoli, P. Yadav, R. Tavakoli and J. Kong, *Adv. Energy Mater.*, 2018, **8**, 1800794.
9 X. Zheng, Y. Hou, C. Bao, J. Yin, F. Yuan, Z. Huang, K. Song, J. Liu, J. Troughton, N. Gasparini, C. Zhou, Y. Lin, D.-J. Xue, B. Chen, A. K. Johnston, N. Wei, M. N. Hedhili, M. Wei, A. Y. Alsalloum, P. Maity, B. Turedi, C. Yang, D. Baran, T. D. Anthopoulos, Y. Han, Z.-H. Lu, O. F. Mohammed, F. Gao, E. H. Sargent and O. M. Bakr, *Nat. Energy*, 2020, **5**, 131–140.
10 M. Kim, J. Jeong, H. Lu, T. K. Lee, F. T. Eickemeyer, Y. Liu, I. W. Choi, S. J. Choi, Y. Jo, H.-B. Kim, S.-I. Mo, Y.-K. Kim, H. Lee, N. G. An, S. Cho, W. R. Tress, S. M. Zakeeruddin, A. Hagfeldt, J. Y. Kim, M. Grätzel and D. S. Kim, *Science*, 2022, **375**, 302–306.
11 D. H. Kim, J. B. Whitaker, Z. Li, M. F. A. M. van Hest and K. Zhu, *Joule*, 2018, **2**, 1437–1451.
12 Z. Fu, M. Xu, Y. Sheng, Z. Yan, J. Meng, C. Tong, D. Li, Z. Wan, Y. Ming and A. Mei, *Adv. Funct. Mater.*, 2019, **29**, 1809129.
13 X. He, J. Chen, X. Ren, L. Zhang, Y. Liu, J. Feng, J. Fang, K. Zhao and S. Liu, *Adv. Mater.*, 2021, **33**, 2100770.
14 E. Y. Choi, J. Kim, S. Lim, E. Han, A. W. Y. Ho-Baillie and N. Park, *Sol. Energy Mater. Sol. Cells*, 2018, **188**, 37–45.
15 S. G. Hashmi, D. Martineau, X. Li, M. Ozkan, A. Tiihonen, M. I. Dar, T. Sarikka, S. M. Zakeeruddin, J. Paltakari, P. D. Lund and M. Grätzel, *Adv. Mater. Technol.*, 2017, **2**, 1600183.
16 S. G. Hashmi, A. Tiihonen, D. Martineau, M. Ozkan, P. Vivo, K. Kaunisto, V. Ulla, S. M. Zakeeruddin and M. Grätzel, *J. Mater. Chem. A*, 2017, **5**, 4797–4802.
17 C. M. Thi Kim, L. Atourki, M. Ouafi and S. G. Hashmi, *J. Mater. Chem. A*, 2021, **9**, 26650–26668.
18 S. G. Hashmi, D. Martineau, M. I. Dar, T. T. T. Myllymäki, T. Sarikka, V. Ulla, S. M. Zakeeruddin and M. Grätzel, *J. Mater. Chem. A*, 2017, **5**, 12060–12067.
19 B. O'Regan and M. Grätzel, *Nature*, 1991, **353**, 737–740.
20 S. Liu, J. Yuan, W. Deng, M. Luo, Y. Xie, Q. Liang, Y. Zou, Z. He, H. Wu and Y. Cao, *Nat. Photonics*, 2020, **14**, 300–305.
21 M. M. Lee, J. Teuscher, T. Miyasaka, T. N. Murakami and H. J. Snaith, *Science*, 2012, **338**, 643–647.
22 M. Kokkonen, P. Talebi, J. Zhou, S. Asgari, S. A. Soomro, F. Elsehrawy, J. Halme, S. Ahmad, A. Hagfeldt and S. G. Hashmi, *J. Mater. Chem. A*, 2021, **9**, 10527–10545.
23 P. Corti, P. Bonomo, F. Frontini, P. Mace and E. Bosch, *Building Integrated Photovoltaics: A Practical Handbook for Solar Buildings*, SUPSI-Becquerel Institute, 2020.
24 H. Michaels, M. Rinderle, R. Freitag, I. Benesperi, T. Edvinsson, R. Socher, A. Gagliardi and M. Freitag, *Chem. Sci.*, 2020, **11**, 2895–2906.
25 K.-L. Wang, Y.-H. Zhou, Y.-H. Lou and Z.-K. Wang, *Chem. Sci.*, 2021, **12**, 11936–11954.
26 *IoT*, **https://sauletech.com/iot/**, accessed January 7, 2022.
27 Y. Rong, Y. Hu, A. Mei, H. Tan, M. I. Saidaminov, S. I. Seok, M. D. McGehee, E. H. Sargent and H. Han, *Science*, 2018, **361**, eaat8235.
28 D. Li, D. Zhang, K. Lim, Y. Hu, Y. Rong, A. Mei, N. Park and H. Han, *Adv. Funct. Mater.*, 2021, **31**, 2008621.
29 Y. Deng, X. Zheng, Y. Bai, Q. Wang, J. Zhao and J. Huang, *Nat. Energy*, 2018, **3**, 560–566.
30 S. Razza, F. Di Giacomo, F. Matteocci, L. Cinà, A. L. Palma, S. Casaluci, P. Cameron, A. D'Epifanio, S. Licoccia, A. Reale, T. M. Brown and A. Di Carlo, *J. Power Sources*, 2015, **277**, 286–291.
31 J. Ali, Y. Li, P. Gao, T. Hao, J. Song, Q. Zhang, L. Zhu, J. Wang, W. Feng, H. Hu and F. Liu, *Nanoscale*, 2020, **12**, 5719–5745.
32 L.-L. Gao, L.-S. Liang, X.-X. Song, B. Ding, G.-J. Yang, B. Fan, C.-X. Li and C.-J. Li, *J. Mater. Chem. A*, 2016, **4**, 3704–3710.
33 B. A. Nejand, P. Nazari, S. Gharibzadeh, V. Ahmadi and A. Moshaii, *Chem. Commun.*, 2017, **53**, 747–750.
34 C. Bi, B. Chen, H. Wei, S. DeLuca and J. Huang, *Adv. Mater.*, 2017, **29**, 1605900.
35 M. Lee, Y. Jo, D. S. Kim and Y. Jun, *J. Mater. Chem. A*, 2015, **3**, 4129–4133.
36 Y. Li, L. Meng, Y. M. Yang, G. Xu, Z. Hong, Q. Chen, J. You, G. Li, Y. Yang and Y. Li, *Nat. Commun.*, 2016, **7**, 1–10.
37 A. Tooghi, D. Fathi and M. Eskandari, *Sci. Rep.*, 2020, **10**, 1–13.
38 Y. Li, M. Cheng, E. Jungstedt, B. Xu, L. Sun and L. Berglund, *ACS Sustainable Chem. Eng.*, 2019, **7**, 6061–6067.
39 P. Li, C. Liang, B. Bao, Y. Li, X. Hu, Y. Wang, Y. Zhang, F. Li, G. Shao and Y. Song, *Nano Energy*, 2018, **46**, 203–211.
40 S. Huang, C. Guan, P. Lee, H. Huang, C. Li, Y. Huang and W. Su, *Adv. Energy Mater.*, 2020, **10**, 2070155.
41 M. Du, X. Zhu, L. Wang, H. Wang, J. Feng, X. Jiang, Y. Cao, Y. Sun, L. Duan and Y. Jiao, *Adv. Mater.*, 2020, **32**, 2004979.
42 D. Burkitt, R. Patidar, P. Greenwood, K. Hooper, J. McGettrick, S. Dimitrov, M. Colombo, V. Stoichkov, D. Richards, D. Beynon, M. Davies and T. Watson, *Sustainable Energy Fuels*, 2020, **4**, 3340–3351.
43 K.-S. Lim, D.-K. Lee, J.-W. Lee and N.-G. Park, *J. Mater. Chem. A*, 2020, **8**, 9345–9354.

44 C. Li, J. Yin, R. Chen, X. Lv, X. Feng, Y. Wu and J. Cao, *J. Am. Chem. Soc.*, 2019, **141**, 6345–6351.
45 P. Zhao, B. J. Kim, X. Ren, D. G. Lee, G. J. Bang, J. B. Jeon, W. Bin Kim and H. S. Jung, *Adv. Mater.*, 2018, **30**, 1802763.
46 S. H. Huang, C. K. Guan, P. H. Lee, H. C. Huang, C. F. Li, Y. C. Huang and W. F. Su, *Adv. Energy Mater.*, 2020, **10**, 1–9.
47 D. Newell, M. Duffy and R. Twohig, in *2014 IEEE Applied Power Electronics Conference and Exposition-APEC 2014*, IEEE, 2014, pp. 3155–3159.
48 S. So, I. Hwang, J. Yoo, S. Mohajernia, M. Mačković, E. Spiecker, G. Cha, A. Mazare and P. Schmuki, *Adv. Energy Mater.*, 2018, **8**, 1800981.
49 X. Yang, J. Xi, Y. Sun, Y. Zhang, G. Zhou and W.-Y. Wong, *Nano Energy*, 2019, **64**, 103946.
50 L. Luo, Y. Zhang, N. Chai, X. Deng, J. Zhong, F. Huang, Y. Peng, Z. Ku and Y.-B. Cheng, *J. Mater. Chem. A*, 2018, **6**, 21143–21148.
51 J. Xiao, Y. Tan, Y. Song and Q. Zheng, *J. Mater. Chem. A*, 2018, **6**, 9074–9080.
52 A. Möllmann, D. Gedamu, P. Vivo, R. Frohnhoven, D. Stadler, T. Fischer, I. Ka, M. Steinhorst, R. Nechache and F. Rosei, *Adv. Eng. Mater.*, 2019, **21**, 1801196.
53 M. Shahiduzzaman, M. I. Hossain, S. Visal, T. Kaneko, W. Qarony, S. Umezu, K. Tomita, S. Iwamori, D. Knipp and Y. H. Tsang, *Nano-Micro Lett.*, 2021, **13**, 1–17.
54 I. Kemerchou, F. Rogti, B. Benhaoua, N. Lakhdar, A. Hima, O. Benhaoua and A. Khechekhouche, *J. Nano- Electron. Phys.*, 2019, 3011.
55 H. U. Chen and S. Yang, in *ECS Meeting Abstracts*, IOP Publishing, 2019, p. 2211.
56 J. Tian, H. Li, H. Wang, B. Zheng, Y. Xue and X. Liu, *Chin. Phys. B*, 2018, **27**, 18810.
57 M. Park, W. Cho, G. Lee, S. C. Hong, M. Kim, J. Yoon, N. Ahn and M. Choi, *Small*, 2019, **15**, 1804005.
58 Y. Zhang, Y. Tu, X. Yang, R. Su, W. Yang, M. Yu, Y. Wang, W. Huang, Q. Gong and R. Zhu, *ACS Appl. Mater. Interfaces*, 2020, **12**, 24905–24912.
59 H. Wang, Y. Zhao, Z. Wang, Y. Liu, Z. Zhao, G. Xu, T.-H. Han, J.-W. Lee, C. Chen and D. Bao, *Nano Energy*, 2020, **69**, 104375.
60 D. Koushik, M. Jošt, A. Dučinskas, C. Burgess, V. Zardetto, C. Weijtens, M. A. Verheijen, W. M. M. Kessels, S. Albrecht and M. Creatore, *J. Mater. Chem. C*, 2019, **7**, 12532–12543.
61 W. Zhu, W. Chai, Z. Zhang, D. Chen, J. Chang, S. Liu, J. Zhang, C. Zhang and Y. Hao, *Org. Electron.*, 2019, **74**, 103–109.
62 J. A. Raiford, S. T. Oyakhire and S. F. Bent, *Energy Environ. Sci.*, 2020, **13**, 1997–2023.
63 S. Seo, S. Jeong, H. Park, H. Shin and N.-G. Park, *Chem. Commun.*, 2019, **55**, 2403–2416.
64 K. Wang, Y. Du, J. Liang, J. Zhao, F. F. Xu, X. Liu, C. Zhang, Y. Yan and Y. S. Zhao, *Adv. Mater.*, 2020, **32**, 2001999.
65 C. Raminafshar, V. Dracopoulos, M. R. Mohammadi and P. Lianos, *Electrochim. Acta*, 2018, **276**, 261–267.
66 M. Xu, W. Ji, Y. Sheng, Y. Wu, H. Cheng, J. Meng, Z. Yan, J. Xu, A. Mei and Y. Hu, *Nano Energy*, 2020, **74**, 104842.
67 L. Chu, R. Hu, W. Liu, Y. Ma, R. Zhang, J. Yang and X. Li, *Mater. Res. Bull.*, 2018, **98**, 322–327.
68 D. Song, L. Y. Hsu, C.-M. Tseng and E. W.-G. Diau, *Mater. Adv.*, 2021, **2**, 754–759.
69 G. Wang, M. A. Adil, J. Zhang and Z. Wei, *Adv. Mater.*, 2019, **31**, 1805089.
70 Q. Kang, B. Yang, Y. Xu, B. Xu and J. Hou, *Adv. Mater.*, 2018, **30**, 1801718.
71 R. Sun, J. Guo, C. Sun, T. Wang, Z. Luo, Z. Zhang, X. Jiao, W. Tang, C. Yang and Y. Li, *Energy Environ. Sci.*, 2019, **12**, 384–395.
72 M. F. Castro, E. Mazzolini, R. R. Sondergaard, M. Espindola-Rodriguez and J. W. Andreasen, *Phys. Rev. Appl.*, 2020, **14**, 34067.
73 L. Zhang, X. Xu, B. Lin, H. Zhao, T. Li, J. Xin, Z. Bi, G. Qiu, S. Guo and K. Zhou, *Adv. Mater.*, 2018, **30**, 1805041.
74 J. Feng, X. Zhu, Z. Yang, X. Zhang, J. Niu, Z. Wang, S. Zuo, S. Priya, S. Liu and D. Yang, *Adv. Mater.*, 2018, **30**, 1801418.
75 Q. Luo, H. Ma, Q. Hou, Y. Li, J. Ren, X. Dai, Z. Yao, Y. Zhou, L. Xiang and H. Du, *Adv. Funct. Mater.*, 2018, **28**, 1706777.
76 Q. Ge, J. Shao, J. Ding, L. Deng, W. Zhou, Y. Chen, J. Ma, L. Wan, J. Yao and J. Hu, *Angew. Chem.*, 2018, **130**, 11125–11131.
77 A. Agresti, B. Berionni Berna, S. Pescetelli, A. Catini, F. Menchini, C. Di Natale, R. Paolesse and A. Di Carlo, *Adv. Funct. Mater.*, 2020, **30**, 2003790.
78 X. Wang, J. Zhang, S. Yu, W. Yu, P. Fu, X. Liu, D. Tu, X. Guo and C. Li, *Angew. Chem., Int. Ed.*, 2018, **57**, 12529–12533.
79 Q.-Q. Chu, B. Ding, J. Peng, H. Shen, X. Li, Y. Liu, C.-X. Li, C.-J. Li, G.-J. Yang and T. P. White, *J. Mater. Sci. Technol.*, 2019, **35**, 987–993.
80 N. Arora, M. I. Dar, S. Akin, R. Uchida, T. Baumeler, Y. Liu, S. M. Zakeeruddin and M. Grätzel, *Small*, 2019, **15**, 1904746.
81 R. Chen, Y. Feng, C. Zhang, M. Wang, L. Jing, C. Ma, J. Bian and Y. Shi, *J. Mater. Chem. C*, 2020, **8**, 9262–9270.
82 S. Alon, M. Sohmer, C. S. Pathak, I. Visoly-Fisher and L. Etgar, *Sol. RRL*, 2021, 2100028.
83 S. M. P. Meroni, Y. Mouhamad, F. De Rossi, A. Pockett, J. Baker, R. Escalante, J. Searle, M. J. Carnie, E. Jewell, G. Oskam and T. M. Watson, *Sci. Technol. Adv. Mater.*, 2018, **19**, 1–9.
84 S. M. P. Meroni, K. E. A. Hooper, T. Dunlop, J. A. Baker, D. Worsley, C. Charbonneau and T. M. Watson, *Energies*, 2020, **13**, 1589.
85 C. Worsley, D. Raptis, S. Meroni, A. Doolin, R. Garcia-Rodriguez, M. Davies and T. Watson, *Energy Technol.*, 2021, **9**, 2100312.
86 L. Yu, J. Jia and G. Yi, *Phys. Status Solidi A*, 2017, **214**, 1600540.
87 P. Venkatachalam, T. Kalaivani and N. Krishnakumar, *Opt. Mater.*, 2019, **94**, 1–8.
88 I. J. E. Mater, *International Journal of Electroactive Materials*, 2017, **5**, 13–18.
89 S. Pang, H. Hu, J. Zhang, S. Lv, Y. Yu, F. Wei, T. Qin, H. Xu, Z. Liu and G. Cui, *Chem. Mater.*, 2014, **26**, 1485–1491.

90 H.-S. Kim, J.-W. Lee, N. Yantara, P. P. Boix, S. A. Kulkarni, S. Mhaisalkar, M. Grätzel and N.-G. Park, *Nano Lett.*, 2013, **13**, 2412–2417.
91 J. Qiu, Y. Qiu, K. Yan, M. Zhong, C. Mu, H. Yan and S. Yang, *Nanoscale*, 2013, **5**, 3245–3248.
92 P. K. Singh, M. Parvaz, S. Ahmed, R. K. Sonker, B. Bhattacharya and Z. H. Khan, *Optik*, 2018, **169**, 166–171.
93 H. Chen and S. Yang, *J. Mater. Chem. A*, 2019, **7**, 15476–15490.
94 M. Hu, L. Liu, A. Mei, Y. Yang, T. Liu and H. Han, *J. Mater. Chem. A*, 2014, **2**, 17115–17121.
95 J. Seo, S. Park, Y. C. Kim, N. J. Jeon, J. H. Noh, S. C. Yoon and S. Il Seok, *Energy Environ. Sci.*, 2014, **7**, 2642–2646.
96 F. Matteocci, S. Razza, F. Di Giacomo, S. Casaluci, G. Mincuzzi, T. M. Brown, A. D'Epifanio, S. Licoccia and A. Di Carlo, *Phys. Chem. Chem. Phys.*, 2014, **16**, 3918–3923.
97 J. H. Heo, H. J. Han, D. Kim, T. K. Ahn and S. H. Im, *Energy Environ. Sci.*, 2015, **8**, 1602–1608.
98 K. Hwang, Y. Jung, Y. Heo, F. H. Scholes, S. E. Watkins, J. Subbiah, D. J. Jones, D. Kim and D. Vak, *Adv. Mater.*, 2015, **27**, 1241–1247.
99 A. Priyadarshi, L. J. Haur, P. Murray, D. Fu, S. Kulkarni, G. Xing, T. C. Sum, N. Mathews and S. G. Mhaisalkar, *Energy Environ. Sci.*, 2016, **9**, 3687–3692.
100 J. H. Heo, M. H. Lee, M. H. Jang and S. H. Im, *J. Mater. Chem. A*, 2016, **4**, 17636–17642.
101 A. Agresti, S. Pescetelli, A. L. Palma, A. E. Del Rio Castillo, D. Konios, G. Kakavelakis, S. Razza, L. Cinà, E. Kymakis and F. Bonaccorso, *ACS Energy Lett.*, 2017, **2**, 279–287.
102 H. Chen, F. Ye, W. Tang, J. He, M. Yin, Y. Wang, F. Xie, E. Bi, X. Yang and M. Grätzel, *Nature*, 2017, **550**, 92–95.
103 G. Jang, H. Kwon, S. Ma, S. Yun, H. Yang and J. Moon, *Adv. Energy Mater.*, 2019, **9**, 1901719.
104 D.-K. Lee, D.-N. Jeong, T. K. Ahn and N.-G. Park, *ACS Energy Lett.*, 2019, **4**, 2393–2401.
105 Z.-L. Tseng, C.-H. Chiang and C.-G. Wu, *Sol. RRL*, 2020, **4**, 1900402.
106 S. Huang, C. Guan, P. Lee, H. Huang, C. Li, Y. Huang and W. Su, *Adv. Energy Mater.*, 2020, **10**, 2001567.
107 Y. Sha, E. Bi, Y. Zhang, P. Ru, W. Kong, P. Zhang, X. Yang, H. Chen and L. Han, *Adv. Energy Mater.*, 2021, **11**, 2003301.
108 G. Tong, D. Son, L. K. Ono, Y. Liu, Y. Hu, H. Zhang, A. Jamshaid, L. Qiu, Z. Liu and Y. Qi, *Adv. Energy Mater.*, 2021, **11**, 2003712.
109 G. Tong, L. K. Ono, Y. Liu, H. Zhang, T. Bu and Y. Qi, *Nano-Micro Lett.*, 2021, **13**, 1–14.
110 H. Zhang, K. Darabi, N. Y. Nia, A. Krishna, P. Ahlawat, B. Guo, M. H. S. Almalki, T.-S. Su, D. Ren, V. Bolnykh, L. A. Castriotta, M. Zendehdel, L. Pan, S. S. Alonso, R. Li, S. M. Zakeeruddin, A. Hagfeldt, U. Rothlisberger, A. Di Carlo, A. Amassian and M. Grätzel, *Nat. Commun.*, 2022, **13**, 89.
111 L. Qiu, S. He, Y. Jiang, D.-Y. Son, L. K. Ono, Z. Liu, T. Kim, T. Bouloumis, S. Kazaoui and Y. Qi, *J. Mater. Chem. A*, 2019, **7**, 6920–6929.
112 L. A. Castriotta, R. Fuentes Pineda, V. Babu, P. Spinelli, B. Taheri, F. Matteocci, F. Brunetti, K. Wojciechowski and A. Di Carlo, *ACS Appl. Mater. Interfaces*, 2021, **13**, 29576–29584.
113 H. Wang, Z. Huang, S. Xiao, X. Meng, Z. Xing, L. Rao, C. Gong, R. Wu, T. Hu, L. Tan, X. Hu, S. Zhang and Y. Chen, *J. Mater. Chem. A*, 2021, **9**, 5759–5768.
114 F. Matteocci, L. Cinà, F. Di Giacomo, S. Razza, A. L. Palma, A. Guidobaldi, A. D'Epifanio, S. Licoccia, T. M. Brown, A. Reale and A. Di Carlo, *Progress in Photovoltaics: Research and Applications*, 2016, **24**, 436–445.
115 M. Yang, Z. Li, M. O. Reese, O. G. Reid, D. H. Kim, S. Siol, T. R. Klein, Y. Yan, J. J. Berry, M. F. A. M. Van Hest and K. Zhu, *Nat. Energy*, 2017, **2**, 1–9.
116 T. Bu, J. Li, F. Zheng, W. Chen, X. Wen, Z. Ku, Y. Peng, J. Zhong, Y. B. Cheng and F. Huang, *Nat. Commun.*, 2018, **9**, 1–10.
117 Z. Liu, L. Qiu, E. J. Juarez-Perez, Z. Hawash, T. Kim, Y. Jiang, Z. Wu, S. R. Raga, L. K. Ono, S. Liu and Y. Qi, *Nat. Commun.*, 2018, **9**, 1–11.
118 E. Bi, W. Tang, H. Chen, Y. Wang, J. Barbaud, T. Wu, W. Kong, P. Tu, H. Zhu, X. Zeng, J. He, S. Kan, X. Yang, M. Grätzel and L. Han, *Joule*, 2019, **3**, 2748–2760.
119 J. Chung, S. S. Shin, K. Hwang, G. Kim, K. W. Kim, D. S. Lee, W. Kim, B. S. Ma, Y. K. Kim, T. S. Kim and J. Seo, *Energy Environ. Sci.*, 2020, **13**, 4854–4861.
120 X. Dai, Y. Deng, C. H. Van Brackle, S. Chen, P. N. Rudd, X. Xiao, Y. Lin, B. Chen and J. Huang, *Adv. Energy Mater.*, 2020, **10**, 1903108.
121 X. Huang, R. Chen, G. Deng, F. Han, P. Ruan, F. Cheng, J. Yin, B. Wu and N. Zheng, *J. Am. Chem. Soc.*, 2020, **142**, 6149–6157.
122 N. Yaghoobi Nia, M. Zendehdel, M. Abdi-Jalebi, L. A. Castriotta, F. U. Kosasih, E. Lamanna, M. M. Abolhasani, Z. Zheng, Z. Andaji-Garmaroudi, K. Asadi, G. Divitini, C. Ducati, R. H. Friend and A. Di Carlo, *Nano Energy*, 2021, **82**, 105685.
123 M. Du, X. Zhu, L. Wang, H. Wang, J. Feng, X. Jiang, Y. Cao, Y. Sun, L. Duan, Y. Jiao, K. Wang, X. Ren, Z. Yan, S. Pang and S. Liu, *Adv. Mater.*, 2020, **32**, 1–10.
124 H. Li, N. Liu, Z. Shao, H. Li, L. Xiao, J. Bian, J. Li, Z. Tan, M. Zhu, Y. Duan, L. Gao, G. Niu, J. Tang, Y. Huang and Z. Yin, *J. Mater. Chem. C*, 2019, **7**, 14867–14873.
125 T. Xue, G. Chen, X. Hu, M. Su, Z. Huang, X. Meng, Z. Jin, J. Ma, Y. Zhang and Y. Song, *ACS Appl. Mater. Interfaces*, 2021, **13**, 19959–19969.
126 F. Bisconti, A. Giuri, R. Suhonen, T. M. Kraft, M. Ylikunnari, V. Holappa, R. Po', P. Biagini, A. Savoini, G. Marra, S. Colella and A. Rizzo, *Cell Rep. Phys. Sci.*, 2021, **2**, 100639.
127 A. Giuri, E. Saleh, A. Listorti, S. Colella, A. Rizzo, C. Tuck and C. Esposito Corcione, *Nanomaterials*, 2019, **9**, 582.
128 Y. Y. Kim, T.-Y. Yang, R. Suhonen, A. Kemppainen, K. Hwang, N. J. Jeon and J. Seo, *Nat. Commun.*, 2020, **11**, 5146.
129 Z. Huang, X. Hu, Z. Xing, X. Meng, X. Duan, J. Long, T. Hu, L. Tan and Y. Chen, *J. Phys. Chem. C*, 2020, **124**, 8129–8139.
130 Md. Shahiduzzaman, K. Yamamoto, Y. Furumoto, K. Yonezawa, K. Hamada, K. Kuroda, K. Ninomiya,

M. Karakawa, T. Kuwabara, K. Takahashi, K. Takahashi and T. Taima, *Org. Electron.*, 2017, **48**, 147–153.
131 M.-R. Ahmadian-Yazdi, A. Rahimzadeh, Z. Chouqi, Y. Miao and M. Eslamian, *AIP Adv.*, 2018, **8**, 025109.
132 R. Sun, Q. Wu, J. Guo, T. Wang, Y. Wu, B. Qiu, Z. Luo, W. Yang, Z. Hu, J. Guo, M. Shi, C. Yang, F. Huang, Y. Li and J. Min, *Joule*, 2020, **4**, 407–419.
133 Z. Liu, L. Qiu, L. K. Ono, S. He, Z. Hu, M. Jiang, G. Tong, Z. Wu, Y. Jiang, D.-Y. Son, Y. Dang, S. Kazaoui and Y. Qi, *Nat. Energy*, 2020, **5**, 596–604.
134 Z. Li, T. R. Klein, D. H. Kim, M. Yang, J. J. Berry, M. F. A. M. van Hest and K. Zhu, *Nat. Rev. Mater.*, 2018, **3**, 18017.
135 S. Tang, Y. Deng, X. Zheng, Y. Bai, Y. Fang, Q. Dong, H. Wei and J. Huang, *Adv. Energy Mater.*, 2017, **7**, 1700302.
136 F. Schackmar, H. Eggers, M. Frericks, B. S. Richards, U. Lemmer, G. Hernandez-Sosa and U. W. Paetzold, *Adv. Mater. Technol.*, 2021, **6**, 2000271.
137 N. Rolston, W. J. Scheideler, A. C. Flick, J. P. Chen, H. Elmaraghi, A. Sleugh, O. Zhao, M. Woodhouse and R. H. Dauskardt, *Joule*, 2020, **4**, 2675–2692.
138 T. M. Schmidt, T. T. Larsen-Olsen, J. E. Carlé, D. Angmo and F. C. Krebs, *Adv. Energy Mater.*, 2015, **5**, 1500569.
139 Y. Deng, E. Peng, Y. Shao, Z. Xiao, Q. Dong and J. Huang, *Energy Environ. Sci.*, 2015, **8**, 1544–1550.
140 A. Agresti, S. Pescetelli, A. L. Palma, A. E. Del Rio Castillo, D. Konios, G. Kakavelakis, S. Razza, L. Cinà, E. Kymakis and F. Bonaccorso, *ACS Energy Lett.*, 2017, **2**, 279–287.
141 R. Patidar, D. Burkitt, K. Hooper, D. Richards and T. Watson, *Mater. Today Commun.*, 2020, **22**, 100808.
142 F. C. Krebs, J. Fyenbo and M. Jørgensen, *J. Mater. Chem.*, 2010, **20**, 8994.
143 B. Zimmermann, H.-F. Schleiermacher, M. Niggemann and U. Würfel, *Sol. Energy Mater. Sol. Cells*, 2011, **95**, 1587–1589.
144 X. Ding, J. Liu and T. A. L. Harris, *AIChE J.*, 2016, **62**, 2508–2524.
145 D. Vak, K. Hwang, A. Faulks, Y.-S. Jung, N. Clark, D.-Y. Kim, G. J. Wilson and S. E. Watkins, *Adv. Energy Mater.*, 2015, **5**, 1401539.
146 D. Lee, Y.-S. Jung, Y.-J. Heo, S. Lee, K. Hwang, Y.-J. Jeon, J.-E. Kim, J. Park, G. Y. Jung and D.-Y. Kim, *ACS Appl. Mater. Interfaces*, 2018, **10**, 16133–16139.
147 J. B. Whitaker, D. H. Kim, B. W. Larson, F. Zhang, J. J. Berry, M. F. A. M. van Hest and K. Zhu, *Sustainable Energy Fuels*, 2018, **2**, 2442–2449.
148 Y.-S. Jung, K. Hwang, Y.-J. Heo, J.-E. Kim, D. Lee, C.-H. Lee, H.-I. Joh, J.-S. Yeo and D.-Y. Kim, *ACS Appl. Mater. Interfaces*, 2017, **9**, 27832–27838.
149 B. Dou, J. B. Whitaker, K. Bruening, D. T. Moore, L. M. Wheeler, J. Ryter, N. J. Breslin, J. J. Berry, S. M. Garner, F. S. Barnes, S. E. Shaheen, C. J. Tassone, K. Zhu and M. F. A. M. van Hest, *ACS Energy Lett.*, 2018, **3**, 2558–2565.
150 F. Mathies, E. J. W. List-Kratochvil and E. L. Unger, *Energy Technol.*, 2020, **8**, 1900991.
151 S.-G. Li, K.-J. Jiang, M.-J. Su, X.-P. Cui, J.-H. Huang, Q.-Q. Zhang, X.-Q. Zhou, L.-M. Yang and Y.-L. Song, *J. Mater. Chem. A*, 2015, **3**, 9092–9097.
152 *Japan's NEDO and Panasonic achieve 16.09% Efficiency for Large-area Perovskite Solar Cell Module | Perovskite-Info*, **https://www.perovskite-info.com/japan-s-nedo-and-panasonic-achieve-1609-efficiency-large-area-perovskite-solar**, accessed January 7, 2022.
153 *Products*, **https://sauletech.com/product/**, accessed January 7, 2022.
154 Z. Yang, C.-C. Chueh, F. Zuo, J. H. Kim, P.-W. Liang and A. K.-Y. Jen, *Adv. Energy Mater.*, 2015, **5**, 1500328.
155 N.-G. Park and K. Zhu, *Nat. Rev. Mater.*, 2020, **5**, 333–350.
156 S.-H. Huang, K.-Y. Tian, H.-C. Huang, C.-F. Li, W.-C. Chu, K.-M. Lee, Y.-C. Huang and W.-F. Su, *ACS Appl. Mater. Interfaces*, 2020, **12**, 26041–26049.
157 D. Bogachuk, S. Zouhair, K. Wojciechowski, B. Yang, V. Babu, L. Wagner, B. Xu, J. Lim, S. Mastroianni, H. Pettersson, A. Hagfeldt and A. Hinsch, *Energy Environ. Sci.*, 2020, **13**, 3880–3916.
158 I. A. Howard, T. Abzieher, I. M. Hossain, H. Eggers, F. Schackmar, S. Ternes, B. S. Richards, U. Lemmer and U. W. Paetzold, *Adv. Mater.*, 2019, **31**, 1806702.
159 F. C. Krebs, *Sol. Energy Mater. Sol. Cells*, 2009, **93**, 394–412.
160 Y. Yu, F. Zhang, T. Hou, X. Sun, H. Yu and M. Zhang, *Sol. RRL*, 2021, **5**, 2100386.
161 N. J. Jeon, J. H. Noh, Y. C. Kim, W. S. Yang, S. Ryu and S. I. Seok, *Nat. Mater.*, 2014, **13**, 897–903.
162 J. Zhang, T. Bu, J. Li, H. Li, Y. Mo, Z. Wu, Y. Liu, X.-L. Zhang, Y.-B. Cheng and F. Huang, *J. Mater. Chem. A*, 2020, **8**, 8447–8454.
163 J. E. Bishop, J. A. Smith and D. G. Lidzey, *ACS Appl. Mater. Interfaces*, 2020, **12**, 48237–48245.
164 A. T. Barrows, A. J. Pearson, C. K. Kwak, A. D. F. Dunbar, A. R. Buckley and D. G. Lidzey, *Energy Environ. Sci.*, 2014, **7**, 2944–2950.
165 K. M. Boopathi, M. Ramesh, P. Perumal, Y.-C. Huang, C.-S. Tsao, Y.-F. Chen, C.-H. Lee and C.-W. Chu, *J. Mater. Chem. A*, 2015, **3**, 9257–9263.
166 M. Ramesh, K. M. Boopathi, T.-Y. Huang, Y.-C. Huang, C.-S. Tsao and C.-W. Chu, *ACS Appl. Mater. Interfaces*, 2015, **7**, 2359–2366.
167 J. G. Tait, S. Manghooli, W. Qiu, L. Rakocevic, L. Kootstra, M. Jaysankar, C. A. Masse de la Huerta, U. W. Paetzold, R. Gehlhaar, D. Cheyns, P. Heremans and J. Poortmans, *J. Mater. Chem. A*, 2016, **4**, 3792–3797.
168 J. E. Bishop, C. D. Read, J. A. Smith, T. J. Routledge and D. G. Lidzey, *Sci. Rep.*, 2020, **10**, 6610.
169 D. Bi, C. Yi, J. Luo, J.-D. Décoppet, F. Zhang, S. M. Zakeeruddin, X. Li, A. Hagfeldt and M. Grätzel, *Nat. Energy*, 2016, **1**, 16142.
170 D. Bi, W. Tress, M. I. Dar, P. Gao, J. Luo, C. Renevier, K. Schenk, A. Abate, F. Giordano, J.-P. Correa Baena, J.-D. Decoppet, S. M. Zakeeruddin, M. K. Nazeeruddin, M. Grätzel and A. Hagfeldt, *Sci. Adv.*, 2016, **2**, e1501170.
171 Y. Y. Kim, T. Yang, R. Suhonen, M. Välimäki, T. Maaninen, A. Kemppainen, N. J. Jeon and J. Seo, *Adv. Sci.*, 2019, **6**, 1802094.

172 F. Hilt, M. Q. Hovish, N. Rolston, K. Brüning, C. J. Tassone and R. H. Dauskardt, *Energy Environ. Sci.*, 2018, **11**, 2102–2113.
173 F. Di Giacomo, S. Shanmugam, H. Fledderus, B. J. Bruijnaers, W. J. H. Verhees, M. S. Dorenkamper, S. C. Veenstra, W. Qiu, R. Gehlhaar, T. Merckx, T. Aernouts, R. Andriessen and Y. Galagan, *Sol. Energy Mater. Sol. Cells*, 2018, **181**, 53–59.
174 C. Liang, P. Li, H. Gu, Y. Zhang, F. Li, Y. Song, G. Shao, N. Mathews and G. Xing, *Sol. RRL*, 2018, **2**, 1700217.
175 L. Vesce, M. Stefanelli and A. Di Carlo, *Energies*, 2021, **14**, 6081.
176 X. Meng, Z. Cai, Y. Zhang, X. Hu, Z. Xing, Z. Huang, Z. Huang, Y. Cui, T. Hu, M. Su, X. Liao, L. Zhang, F. Wang, Y. Song and Y. Chen, *Nat. Commun.*, 2020, **11**, 3016.
177 C. Worsley, D. Raptis, S. M. P. Meroni, R. Patidar, A. Pockett, T. Dunlop, S. J. Potts, R. Bolton, C. M. E. Charbonneau, M. Carnie, E. Jewell and T. Watson, *Mater. Adv.*, 2022, **3**, 1125–1138.
178 W. Xiang, S. Liu and W. Tress, *Energy Environ. Sci.*, 2021, **14**, 2090–2113.
179 M. Jeevaraj, S. Sudhahar and M. K. Kumar, *Mater. Today Commun.*, 2021, **27**, 102159.
180 M. I. Asghar, J. Zhang, H. Wang and P. D. Lund, *Renewable Sustainable Energy Rev.*, 2017, **77**, 131–146.
181 Y. Han, S. Meyer, Y. Dkhissi, K. Weber, J. M. Pringle, U. Bach, L. Spiccia and Y.-B. Cheng, *J. Mater. Chem. A*, 2015, **3**, 8139–8147.
182 L. Shi, M. P. Bucknall, T. L. Young, M. Zhang, L. Hu, J. Bing, D. S. Lee, J. Kim, T. Wu and N. Takamure, *Science*, 2020, **368**, eaba2412.
183 T. Bu, J. Li, F. Zheng, W. Chen, X. Wen, Z. Ku, Y. Peng, J. Zhong, Y. B. Cheng and F. Huang, *Nat. Commun.*, 2018, **9**, 1–10.
184 N. Y. Nia, M. Zendehdel, M. Abdi-Jalebi, L. A. Castriotta, F. U. Kosasih, E. Lamanna, M. M. Abolhasani, Z. Zheng, Z. Andaji-Garmaroudi and K. Asadi, *Nano Energy*, 2021, **82**, 105685.
185 A. Mei, X. Li, L. Liu, Z. Ku, T. Liu, Y. Rong, M. Xu, M. Hu, J. Chen and Y. Yang, *science*, 2014, **345**, 295–298.
186 Y. Rong, Y. Hu, A. Mei, H. Tan, M. I. Saidaminov, S. Il Seok, M. D. McGehee, E. H. Sargent and H. Han, *Science*, 2017, **361**, 1–7.
187 Y. Hu, S. Si, A. Mei, Y. Rong, H. Liu, X. Li and H. Han, *Sol. RRL*, 2017, **1**, 1600019.
188 S. G. Hashmi, M. Ozkan, D. Martineau, X. Li, S. M. Zakeeruddin and M. Graetzel, Method for inkjet printing an organic–inorganic perovskite, *US Pat.* 11177440 B2, 2018.
189 A. A. Asif, R. Singh and G. F. Alapatt, *J. Renewable Sustainable Energy*, 2015, **7**, 43120.
190 *Saule Technologies Launches The First Production Line*, **https://sauletech.com/launching-production-line/**, accessed January 7, 2022.
191 *Unique Perovskite Solar Pilot Line | Oxford PV*, **https://www.oxfordpv.com/tandem-cell-production**, accessed January 7, 2022.
192 Swift Solar, *Next Generation Lightweight and Flexible Solar Technology*, **https://www.swiftsolar.com/**, accessed January 7, 2022.
193 Technology, **https://sauletech.com/technology/**, accessed January 7, 2022.
194 Technology – Solaires Entreprises Inc, **https://www.solaires.net/technology/solarink**, accessed January 7, 2022.
195 E. Kobayashi, R. Tsuji, D. Martineau, A. Hinsch and S. Ito, *Cell Rep. Phys. Sci.*, 2021, 100648.
196 P. Fu, W. Qin, S. Bai, D. Yang, L. Chen, X. Guo and C. Li, *Nano Energy*, 2019, **65**, 104009.
197 M. Yang, Z. Li, M. O. Reese, O. G. Reid, D. H. Kim, S. Siol, T. R. Klein, Y. Yan, J. J. Berry, M. F. A. M. Van Hest and K. Zhu, *Nat. Energy*, 2017, **2**, 1–9.
198 J. Kim, J. S. Yun, Y. Cho, D. S. Lee, B. Wilkinson, A. M. Soufiani, X. Deng, J. Zheng, A. Shi and S. Lim, *ACS Energy Lett.*, 2017, **2**, 1978–1984.
199 Z.-L. Tseng, C.-H. Chiang and C.-G. Wu, *Sol. RRL*, 2020, **4**, 1900402.
200 H. Chen, F. Ye, W. Tang, J. He, M. Yin, Y. Wang, F. Xie, E. Bi, X. Yang and M. Grätzel, *Nature*, 2017, **550**, 92–95.
201 Y. Deng, X. Zheng, Y. Bai, Q. Wang, J. Zhao and J. Huang, *Nat. Energy*, 2018, **3**, 560–566.
202 F. De Rossi, J. A. Baker, D. Beynon, K. E. A. Hooper, S. M. P. Meroni, D. Williams, Z. Wei, A. Yasin, C. Charbonneau and E. H. Jewell, *Adv. Mater. Technol.*, 2018, **3**, 1800156.
203 J. Feng, Y. Jiao, H. Wang, X. Zhu, Y. Sun, M. Du, Y. Cao, D. Yang and S. F. Liu, *Energy Environ. Sci.*, 2021, **14**, 3035–3043.
204 Z. Ouyang, M. Yang, J. B. Whitaker, D. Li and M. F. A. M. van Hest, *ACS Appl. Energy Mater.*, 2020, **3**, 3714–3720.
205 L. A. Castriotta, M. Zendehdel, N. Yaghoobi Nia, E. Leonardi, M. Löffler, B. Paci, A. Generosi, B. Rellinghaus and A. Di Carlo, *Adv. Energy Mater.*, 2022, **12**, 2103420.
206 M. Fenske, C. Schultz, J. Dagar, F. U. Kosasih, A. Zeiser, C. Junghans, A. Bartelt, C. Ducati, R. Schlatmann, E. Unger and B. Stegemann, *Energy Technol.*, 2021, **9**, 2000969.
207 K. G. Brooks and M. K. Nazeeruddin, *Adv. Energy Mater.*, 2021, **11**, 2101149.
208 C. Trudeau, P. Beaupré, M. Bolduc and S. G. Cloutier, *npj Flexible Electron.*, 2020, **4**, 34.
209 Y. Wang, C. Duan, P. Lv, Z. Ku, J. Lu, F. Huang and Y.-B. Cheng, *Natl. Sci. Rev.*, 2021, nwab075.
210 A. Karavioti, D. A. Chalkias, G. Katsagounos, A. Mourtzikou, A. N. Kalarakis and E. Stathatos, *Electronics*, 2021, **10**, 1904.
211 S. Högnabba, Master thesis, Aalto University, 2021.

